Id genes are required for morphogenesis and cellular patterning in the developing mammalian cochlea

Susumu Sakamoto[1,2], Tomoko Tateya[1,3]*, Koichi Omori[1], and Ryoichiro Kageyama[2,4,5,6]*

[1]Department of Otolaryngology - Head and Neck Surgery, Kyoto University Graduate School of Medicine, Kyoto 606-8507, Japan: [2]Institute for Frontier Life and Medical Sciences, Kyoto University, Kyoto 606-8507, Japan; Kyoto University of Advanced Science, Kyoto 615-8577; [4]Graduate School of Medicine, Kyoto University, Kyoto 606-8501, Japan; [5]Graduate School of Biostudies, Kyoto University, Kyoto 606-8501, Japan; [6]Institute for Integrated Cell-Material Sciences (iCeMS), Kyoto University, Kyoto 606-8501, Japan

*To whom correspondence should be addressed:

E-mail: t_tateya@ent.kuhp.kyoto-u.ac.jp or rkageyam@infront.kyoto-u.ac.jp

Abstract

Inhibitor of differentiation and DNA-binding (Id) proteins, Id1 to Id4, function in the regulation of cellular proliferation and differentiation. Id proteins have been shown to interact with bHLH proteins and other proteins involved in regulating cellular proliferation and differentiation, suggesting a widespread regulatory function. *Id1-3* are known to be expressed in the prosensory domain of developing cochlea. However, the roles of *Id* genes in cochlear development are not fully elucidated. The deficiency of any of the *Id1-3* genes individually has little effect on the cochlear development, and therefore the functional redundancy among these genes have been presumed to explain the absence of phenotype. Here, we show that conditional knockout of *Id1/2/3* genes (*Id* TKO) causes major defects in morphogenesis and cellular patterning in the development of mammalian cochlea. *Id* TKO cochlea was 82% shorter than control, and both decreased proliferation and increased cell death caused the hypomorph. Sox2-positive prosensory domain was formed in *Id* TKO cochlea, but the formation of the medial-lateral (central-peripheral) axis was disturbed; the boundary between the medial and lateral compartments in the prosensory domain was partially doubled; the number of inner hair cells per unit length increased, and the number of outer hair cells decreased. Furthermore, the lateral non-sensory compartment expressing *Bmp4* and *Lmo3* was missing. Thus, the patterning of the lateral epithelium was more affected than the medial epithelium. These results suggested that *Id* genes are crucial for morphogenesis of the cochlea duct and patterning of the lateral epithelium in the developing cochlea. Further analyses by quantitative RT-PCR and immunostaining using cochlear explants with a Bmp pathway inhibitor revealed that the Bmp-Id pathway originates from the lateral non-sensory compartment and promotes outer hair cell differentiation.

Introduction

The cochlea is the organ for hearing perception in the inner ear, and houses the cochlear duct that coils around the conical shaped central axis, the modiolus. The mouse cochlear duct emerges as a ventral out-pocketing from the otocyst around E11 (Morsli et al., 1998) and begins to coil by E12 (Kelley, 2006). As the cochlear duct extends, a subset of cells within the dorsal half of the duct, typically referred to as the floor, begins to develop as the primordium of the organ of Corti, termed the prosensory domain. At E11.5, Sox2 is broadly expressed in the prosensory domain under the effect of lateral induction by Notch signaling (Dabdoub et al., 2008). At E12.5, different sets of genes begin to be expressed across the medial-lateral axis. The Sox2-positive prosensory domain, which is the primordium of the organ of Corti, is flanked by two molecularly distinct non-sensory domains, a medial domain expressing *Fgf10,* which develops into Kölliker's organ, and a lateral domain expressing *Bmp4*, which becomes the outer sulcus (Ohyama et al., 2010). The extending cochlear duct more than doubles its length between E12.5 and P0, indicating significant growth during this time period (Morsli et al., 1998; May-Simera and Kelley, 2012). However, while nonsensory cells within the cochlear duct continue to proliferate during this period, the prosensory domain between Fgf10-positive Kölliker's organ and Bmp4-positive outer sulcus expresses $p27^{Kip1}$ becomes postmitotic between E13 and E14 (Chen et al., 2002; Chen & Segil, 1999; Ruben, 1967; Wang et al., 2005). Afterwards, hair cells and supporting cells differentiate from $p27^{Kip1}$-positive prosensory domain (Kiernan et al., 2005). Hair cells and supporting cells in the cochlea compose the sensory epithelium, called the organ of Corti, which is a well-ordered organ for hearing and extends along the cochlear duct. There are two types of hair cells in the organ of Corti; inner hair cells (IHCs) located at the medial (modiolar) side and outer hair cells (OHCs) located at the lateral (peripheral) side. IHCs detect sound and transmit the signal to the brain via the auditory nerve while OHCs perform a signal-amplifying role. IHCs form a single row and OHCs form three rows. The tunnel of Corti which is formed by two rows of pillar cells, a specific subtype of SC, separates OHCs from IHCs. These highly organized structure in the organ of Corti is indispensable for normal hearing.

Compartment formation across the medial-lateral axis and the induction of IHCs and OHCs are the important processes of the organ of Corti development controlled by signaling pathways, such as the Wnt pathway, which affects the medial side of the cochlear duct floor, and the Bmp pathway, which affects the lateral side of the cochlear duct floor (Groves and Fekete., 2012; Munnamalai and Fekete., 2016; Puligilla et al.,2007; Ohyama et al., 2010). The analysis of compound mouse mutants for the *Alk3* and *Alk6* type I Bmp receptors showed that in the absence of BMP signaling, the majority of the floor in mutant cochlear duct became Kölliker's organ ($Fgf10^{+}$, $Jag1^{+}$, and $Lfng^{+}$), the non-sensory domain medial to prosensory domain, whereas the marker of the outer sulcus *Bmp4* was entirely absent (Ohyama et al., 2010). These results suggest that Bmp signaling is necessary for

establishing the prosensory and lateral non-sensory domains.

Studies in a mouse model suggest that many genes currently known to be associated with hearing impairment play important roles in embryogenesis. Therefore, the investigation of mouse cochlear development provides a rich context for understanding the functions of genes implicated in hearing loss, and we have focused on the function of *Inhibitors of differentiation and DNA binding* (*Id*) genes on cochlear development. Id proteins (Id1, Id2, Id3, and Id4) are small polypeptides harboring a helix-loop-helix (HLH) motif, which are known to mediate dimerization with other basic HLH (bHLH) proteins, primarily E proteins. Because Id proteins do not possess the basic region adjacent to the HLH motif necessary for DNA binding, Id proteins inhibit the function of heterodimers between E proteins and tissue-specific bHLH proteins. Id proteins have been shown to interact with not only bHLH proteins but also other transcription factors such as Ets family members (ELKs) and paired box family (PAXs) (Yates et al., 1999; Chen et al., 2015; Roberts et al., 2001). Id proteins oppose the antiproliferative effects of tumour suppressor proteins such as p16INK4a and Rb and to stimulate proliferation (Lasorella et al., 2000; Ouyang et al., 2002; Lee et al., 2003). Thus, Id proteins have been thought to have a widespread function by regulating the cross-talk between the signaling pathways involved in cellular proliferation and differentiation. For instance, *Id* genes are well-known direct targets of Bmp signaling in various biological contexts (Hollnagel et al., 1999; Korchynskyi et al., 2002; López-Rovira et al., 2002). *Id* genes reportedly play important roles in the development of various organs (Peng et al., 2004; Vinals et al., 2004; Samanta and Kessler., 2004), however, there have been no reports of loss-of-function studies to investigate the function of *Id* genes on cochlear development. Mice with targeted deletions of *Id1*, *Id2*, and *Id3* have been produced (Yan et al., 1997; Lyden et al., 1999; Yokota et al., 1999), but the individual null mutants have very few abnormalities; none of them is associated with hearing deficit, and relatively subtle effects of the inactivation of a single *Id* gene are presumed to be the result of compensation by other *Id* genes (Jones et al., 2006). *Id1* and *Id3* double mutant embryos die at approximately E12 (Lyden et al., 1999), too early to observe the effects of Id inactivation on cochlear development. Conditional compound deletion of *Id* genes in the developing cochlea should be analyzed to understand fully the functions of *Id* proteins in the development of the cochlea, but it has not been done yet.

Jones et al. performed gain-of-function study using cochlear explants established at mouse embryonic day 13 and reported that overexpression of *Id* genes in prosensory cells during hair cell differentiation inhibited these cells from developing as hair cells. These results indicated that *Ids* negatively regulate the *Atoh1* function and hair cell differentiation in the developing cochlea, because the bHLH transcription factor Atoh1 is necessary and sufficient for differentiation of both IHCs and OHCs (Bermingham et al., 1999; Zheng and Gao, 2000). However, the roles of Id proteins in the growth and differentiation of the cochlear epithelium at an earlier stage (before E13) remain to be

elucidated.

In this study, we first investigated the functions of *Id* genes in the developing cochlear epithelium by generating *Id1*, *Id2*, and *Id3* (*Id1-3*) compound mutants, including *Id1;Id2;Id3* triple conditional knockout (*Id* TKO) mice, where Cre-recombinase starts functioning at E11.5 (Tateya et al., 2011). Our results suggested that *Id1–3* are cooperatively regulate the morphogenesis and cellular patterning of the lateral epithelium in the developing cochlea; *Id* TKO cochlea was hypomorphic, and formation of the lateral compartments was disturbed in *Id* TKO cochlear epithelium. We also showed that *Id1–3* are positively regulated by Bmp signaling, and that the Bmp-Id pathway originating from the lateral non-sensory compartment promotes OHC differentiation.

Results

Id gene expression in the developing cochlear epithelium

We first examined *Id* gene expression in the developing cochlear epithelium. At E12.5, three distinct compartments, i.e., an *Fgf10*$^{+}$ medial non-sensory domain, a Sox2^{+} prosensory domain, and a *Bmp4*$^{+}$ lateral non-sensory domain, were about to form along the medial-lateral axis in the floor of the mouse cochlear duct; however, the boundaries of these compartments were obscure at this stage (Fig 1A–C,O). *Id1–3* were co-expressed broadly in the floor of the cochlear duct, including the *Fgf10*$^{+}$, Sox2^{+}, and *Bmp4*$^{+}$ domains (Fig 1D–F). The intensity of *Id1–3* expression was strongest in the lateral side and gradually became weaker toward the medial side (Fig 1D–F,O), as previously reported for *Id2* expression (Ohyama et al., 2010). In contrast, *Id4* was barely expressed lateral to the *Bmp4*-positive domain (Fig 1G). At E13.5, cells in the prosensory domain exited the cell cycle and expressed p27^{kip1} (Fig 1H). The boundaries of the three compartments labeled by *Fgf10*, Sox2;p27^{kip1}, and *Bmp4* became clear at this stage (Fig 1H–J,O). *Id1–3* were expressed continuously in the floor of the cochlear duct (Fig 1K–M), whereas *Id4* was expressed in the roof of the cochlear duct (Fig 1N). At E15.5, not only *Id1–3* but also *Id4* were intensely expressed in developing supporting cells around the differentiating hair cells where *Id* genes were downregulated, and the gradient of *Id1–3* expression from the lateral to medial side became unclear (Fig. S1A-F). At E18.5, after hair cell specification, the expression of *Id* genes was restricted to supporting cells (Fig. S1G-K and S1G'-K').

Id1-3 cooperatively regulate the morphogenesis of the cochlear duct

Id genes are known to have redundant roles in heart and T-cell development (Cunningham et al. 2017; Miyazaki et al. 2015). Due to similar expression patterns of *Id1–3* at E12.5 and E13.5 in the floor of the cochlear duct, we assumed that *Id1–3* had functionally redundant roles in cochlear

development. To elucidate their roles in this process, we used not only *Id1*$^{-/-}$ and *Id2*$^{-/-}$ mice but also *Id3*$^{f/f}$ and *Emx2*$^{cre/+}$ mice to ablate *Id3* expression in all epithelial cells of the cochlear duct from E11.5 and to generate *Id* TKO mice (Tateya et al. 2011).

We compared the cochlear length among the *Id* mutants by F-actin staining with phalloidin. The lengths of *Id1*$^{-/-}$ and *Id1*$^{-/-}$*;Id3*$^{f/f}$*;Emx2*$^{cre/+}$ (*Id1;Id3* double knockout [DKO]) cochleae were similar to that of wild-type cochleae (Fig. 2A,B). In contrast, the lengths of *Id2*$^{-/-}$ and *Id1*$^{-/-}$*Id2*$^{-/-}$ (*Id1Id2* DKO) cochleae were 12% and 35% shorter, respectively, than wild-type cochleae (Fig 2A,B). Moreover, the cochlea of *Id1*$^{-/-}$*;Id2*$^{-/-}$*;Id3*$^{f/f}$*;Emx2*$^{cre/+}$ (*Id* TKO) mice was 82% shorter than that of wild-type mice (Fig 2A,B). These results suggest that *Id2* is responsible for adequate cochlear growth, and that *Id1* and *Id3* partially compensate for the function of *Id2* in cochlear growth.

Id1$^{-/-}$ or *Id1*$^{+/-}$*;Id3*$^{+/-}$ mutants had a normal cochlear length and hair cell patterning, and therefore these mutants were regarded as controls. We presumed that the decreased cochlear length of *Id* compound mutants was caused by a reduction of cell proliferation, increase of cell death, or both. To examine this hypothesis, E12.5 *Id* TKO and control cochleae were analyzed at 2 h after EdU injection by immunostaining for EdU and cleaved caspase-3 (C-cas3). In the Sox2-positive prosensory domain, the number of EdU-incorporating cells in *Id* TKO cochlea decreased compared to that in control cochlea (Fig 2C–E), indicating reduced proliferation. Moreover, at E12.5 and E14.5, the cochlear duct of *Id* TKO mice had more C-cas3-positive apoptotic cells, although no apoptotic cells were observed in the control cochlear duct (Fig 2F–I). These apoptotic cells were located lateral to the p27^{kip1}-positive prosensory domain at E12.5 and E14.5 (Fig 2F–I). Taken together, these results indicated that deletion of *Id1–3* led to a decrease of cell proliferation in the sensory epithelium and an increase of cell death in the lateral non-sensory epithelium of the cochlear duct.

Among the *Id* compound mutants, *Id* TKO cochlear duct had severe morphological abnormalities in addition to the shortest cochlear length. We performed immunolabeling of E-Cadherin and Sox2 using whole-mounted cochleae for three dimensional visualization of the cochlear epithelium. All cochlear epithelial cells were E-cad–positive, except for IHCs and the nonsensory Kolliker's organ domain close to the IHCs (Simonneau et al., 2003), and therefore most of the cochlear epithelium can be visualized by co-labelling of E-Cadherin with Sox2. The control cochlear duct was coiled around the spiral ganglion and drawn in a regular arc (Fig 2J, Movie 1), whereas the *Id* TKO cochlear duct was warped and distorted with expansion and constriction (Fig 2K–L', Movies 2-3). The inner ear of *Id* TKO mice retained the cochleovestibular ganglion at the medial side, but the cochlear duct was not coiled (Fig 2K,L, Movie 2-3). It was noteworthy that the deformation of the shape of *Id* TKO cochlear epithelium was variable between individuals and between the left and right ears, and therefore, the deformation seemed to occur rather randomly. Similar to the whole cochlear epithelium, Sox2-positive sensory epithelium of *Id* TKO mice showed

irregularly expanding and narrowing patterns along the cochlear duct (Fig 2K,K',L,L', Movies 2-3). These results suggested that cochlear morphogenesis was severely disturbed in the absence of all *Id1-3* genes.

Medial-lateral patterning of cochlear epithelium is disturbed in *Id* TKO cochleae

To examine the functions of *Id1–3* on cellular differentiation in developing cochleae, we analyzed control and *Id* TKO cochlear epithelium at E17.5 and E18.5 by immunolabeling with hair cell and supporting cell markers. In the control cochlea, myosin VIIA-positive hair cells were arranged to form one row of IHCs and three rows of OHCs (Fig 3A,D). These IHCs and OHCs were separated by $p75^{NTR}$-positive pillar cells, a specific subtype of supporting cells, in the control (Fig 3A, asterisk, D, arrowhead, and D', Movie 4). In the surface view of control cochlear epithelium, $p75^{NTR}$-positive pillar cells appeared as a straight-line boundary between the medial compartment including IHCs and the lateral compartment including OHCs (Fig 3A). In contrast, *Id* TKO cochlea showed severe disorganization of $p75^{NTR}$-positive pillar cells; *Id* TKO cochlea had one or a few rows of hair cells at the medial side of $p75^{NTR}$-positive pillar cells (Fig 3B,C,E,F). In some cases, the $p75^{NTR}$-positive pillar cell rows were duplicated (Fig 3B, asterisks, and 3F, arrowheads, Movie 5) and hair cells were found occasionally between such duplicated $p75^{NTR}$-positive pillar cell rows (Fig 3B,F). Hair cells were sporadically present at the lateral side of $p75^{NTR}$-positive pillar cells (Fig 3B,C,E,E',F,F'). We analyzed *Id* TKO cochlea further by *in situ* hybridization with *Fgf8*, a marker specific to IHCs. There was one row of *Fgf8* positive IHCs in the control cochlea (Fig 3G,H, asterisks). In contrast, in *Id* TKO mice, most hair cells were positive for *Fgf8* (Fig 3I,J, asterisks). We next analyzed the number of IHCs and the total number of hair cells in the cochleae of control and *Id* TKO mice at E18.5. The hair cells located inside of $p75^{NTR}$-positive pillar cells were defined as IHCs and the other hair cells located outside of ~~and between~~ the row of $p75^{NTR}$-positive pillar cells adjacent to IHCs were defined as OHCs. In the cochleae of *Id* TKO mice, the number of IHCs per unit length increased significantly, however the number of OHCs and the total number of hair cells per unit length decreased significantly (Fig 3K).

Next, we analyzed E17.5 and E18.5 control and *Id* TKO cochleae by immunostaining for Prox1. It was reported that developing outer hair cells and supporting cells transiently express Prox1, whereas by E18, Prox1 expression becomes restricted to pillar cells and Deiters' cells, specific subtypes of supporting cells surrounding OHCs (Bermingham-McDonogh et al., 2006). In the control, Prox1-positive supporting cells were located next to OHCs (Fig 4A, B, D, D'), while those in the most medial row were $p75^{NTR}$-positive pillar cells (see Fig 3D). In contrast, in *Id* TKO cochlea, Prox1-positive supporting cells were partially present at the lateral side of myosin VIIA-positive hair cells (Fig 4C,E,E',F,F').

Id TKO cochlea loses the lateral non-sensory compartment expressing *Bmp4* and *Lmo3*

We next examined the expression of non-sensory regional markers both medial and lateral to the organ of Corti in control and *Id* TKO cochleae at E16.5. In the mid-basal turn of control cochlea, myosin VI-positive IHCs and OHCs were present and accompanied with Sox2- and $p27^{kip1}$-positive developing supporting cells (Fig 5A,D). In the control, *Fgf10* and *Jag1* were specifically expressed in the greater epithelial ridge (GER), which extends from the medial ridge of the cochlear duct to a notch in the developing pillar cell region (Kelley., 2007) (Fig 5B,C), while *Bmp4* and *Lmo3* were expressed in the non-sensory domain lateral to the developing organ of Corti (Fig 5I,J). In *Id* TKO cochlear epithelium, myosin VI-positive hair cells were present in the region medial to $p27^{kip1}$-positive supporting cells, which contained Sox2-positive supporting cells (Fig 5E,H,M). Similar to the control, *Fgf10* and *Jag1* expression occurred in the region medial to the myosin VI- and $p27^{kip1}$-positive developing organ of Corti (Fig 5F,G). However, *Bmp4* and *Lmo3* expression was not detected in *Id* TKO cochlea, indicating that the lateral non-sensory compartment was absent in the mutant mice (Fig 5K,L).

To examine further the non-sensory region of *Id* TKO cochlea, we examined *Lmo4* and *Lmx1a*. *Lmo4* was expressed in the control GER, developing hair cells, and primordial spiral prominence, which is lateral to the $Bmp4^{+}$-positive non-sensory domain at the lateral wall of the cochlear duct at E16.5 (Fig. S2A and S2A') (Deng et al. 2014). On the other hand, it was not expressed in the lateral non-sensory domain (Fig. S2A and S2A'). *Lmo4* was expressed throughout the floor of the *Id* TKO cochlear duct, suggesting that *Id* TKO cochlea lacked the lateral non-sensory domain (Fig. S2B). *Lmx1a* was expressed in the control non-sensory region, except for the GER, organ of Corti, and lateral non-sensory domain (Fig. S2C and S2C') (Huang et al. 2008). In *Id* TKO cochlea, *Lmx1a* expression was maintained (Fig. S2D). These results suggested that *Id1–3* deletion reduced the lateral non-sensory domain while the medial non-sensory domain was maintained.

Id1–3 are positively regulated by Bmp signaling in the developing cochlear epithelium

The expression pattern of *Id1–3*, showing a gradient from the lateral to medial side of cochlear epithelium at E12.5 and E13.5 (Fig 1D-F, K-M), suggested that *Id1–3* function in the formation of the lateral part of cochlear duct. It was shown previously that *Id* genes are regulated by Bmp and Wnt signaling (Kamaid et al. 2010; Ohyama et al., 2010), but it was not clear whether *Id1–3* are all positively regulated by Bmp4 signaling and negatively regulated by Wnt signaling in the mouse cochlear epithelium. To reinforce the relationship between Bmp4 signaling and *Id1–3* expression, we examined the effect of Bmp4 and Noggin (Bmp antagonist) on *Id1–3* expression. E13.5 cochlear epithelium was cultured with different concentrations of Bmp4 or Noggin for 6 h,

and *Id1–3* transcripts were measured by quantitative reverse transcription PCR (RT-qPCR). *Id1–3* transcripts were significantly upregulated after Bmp4 treatment in a dose-dependent manner (Fig. S3A). Conversely, *Id1–3* transcripts were significantly downregulated after Noggin (Bmp antagonist) and CHIR99021 (Wnt activator) treatment (Fig. S3B and S3C). These results indicated that *Id1–3* expression is positively regulated by Bmp signaling and negatively regulated by Wnt signaling.

Inhibition of Bmp4 signaling suppresses *Id1-3* and *Bmp4* expression and OHC differentiation in the developing cochlear epithelium.

The decrease of OHCs in *Id* TKO mutants suggested the involvement of Ids in the Bmp signaling that is required for OHC development. To confirm this notion, we performed an *ex vivo* cochlear culture experiment with LDN193189, a Bmp type I receptor inhibitor. In order to examine the inhibitory effect of LDN193189 on Bmp signaling, we analyzed the transcript levels of *Id1–3* and *Bmp4* in E13.5 cochlear epithelium after culture for 24 h. The expression levels of *Hey1* and *Hey2*, which are known as downstream factors of SHH signaling (Benito-Gonzalez et al., 2014) in cochlear epithelium cultured for 24 h with 400nM LDN193189 did not change, however we found the significant downregulation of *Id1–3* and *Bmp4* expression in cochlear epithelium cultured for 24 h with 400nM LDN193189 (Fig 6A). Next, cochlear explants prepared from E13.5 embryos were cultured with 400nM LDN193189 for 3 days (Fig 6B). The explants were fixed and analyzed by immunostaining for Sox2 and myosin VIIA to visualize the prosensory domain and hair cells, respectively. We found a decrease of OHCs at the basal turn of cochlear explants cultured with 400nM LDN193189, compared to the control (Fig 6C, D). As it was still not clear whether OHC differentiation was completely inhibited or just delayed by the inhibition of Bmp signaling, we performed cochlear explant cultures without LDN193189 for an extra 2 days after 3 days of LDN193189 treatment. The explants were analyzed for hair cell and supporting cell markers. In cochlear explants cultured with 400nM LDN193189, the number of Prox1-positive supporting cells did not decrease (Fig 6I,J,K,L), whereas that of OHCs decreased at both the apical and basal turns (Fig 6E,F,G,H), indicating that blocking the Bmp pathway inhibited OHC differentiation. Thus, cochlear explants cultured with a Bmp inhibitor partially mimicked the phenotype of *Id* TKO mice, suggesting that the Bmp-Id pathway is necessary for OHC differentiation.

Bmp4 signaling was inactivated in *Id* TKO cochleae by up-regulation of Grem1, a potential antagonist of Bmp4

We next performed RNA-sequencing (Seq) analysis using E16.5 control and *Id* TKO cochlear sensory epithelium to understand further the roles of *Id* genes in cochlear duct development. Many genes were differentially expressed between the control and *Id* TKO cochlear

sensory epithelium (Tables S1 and S2), and gene ontology (GO) analysis revealed that the genetic profiles of control and *Id* TKO cochleae had distinct molecular properties. In *Id* TKO cochlear epithelium, the properties in the GO categories of cell proliferation, response to BMP, and regulation of the Bmp signaling pathway were downregulated (Fig. S4A). Pathway analysis showed that Bmp signaling pathway-related genes, Chrd, Sostdc1, Nog and Fst were downregulated; however only *Grem1*, a Bmp antagonist (Zúñig et al., 1999), was significantly upregulated (Figs. S4B and S5). The expression patterns and functions of Grem1 in the developing cochlear epithelium have not been identified; therefore, we performed *in situ* hybridization for *Grem1* in *Id* TKO and control littermates to explore its expression pattern. At E14.5, *Grem1* expression was very low in the control cochlear epithelium (Fig. S4C and S4C'). However, *Grem1* was upregulated throughout the cochlear epithelium of *Id* TKO mutants (Fig. S4D and S4D'). At E16.5, *Grem1* was present in control cochlear epithelium; more strongly expressed in the GER and weakly expressed in the organ of Corti, suggesting that there is an inverse correlation between *Grem1* and *Id1–3* expression patterns (Fig. S4E and S4E'). Indeed, widespread *Grem1* expression was detected throughout the cochlear epithelium of *Id* TKO mutants at E16.5 (Fig. S4F and S4F'), suggesting that deletion of *Id1–3* led to the upregulation of *Grem1* in the cochlear epithelium. Next, we examined the effect of Grem1 on the cochlear epithelium by culturing cochlear explants prepared from E13.5 embryos with recombinant Grem1 for 6 h. RT-qPCR analysis showed that *Id1–3* and *Bmp4* expression was significantly decreased in sensory epithelium treated with recombinant Grem1, compared with the control (Fig. S4G). Taken together, these results indicated that *Id1–3* maintain *Bmp4* expression by inhibiting the expression of *Grem1*.

Relationship between *Id* and *Atoh1*

As mentioned above, it was reported that prosensory cells were inhibited from developing as hair cells by overexpression of *Id* genes during the time period for hair cell differentiation, and it was presumed that *Id* genes negatively regulate the expression of Atoh1 and hair cell differentiation in the developing cochlea (Jones et al., 2006). Our results showed that Atoh1-positive cells were present (Fig 7A, B), and that hair cell differentiation occurred in E14.5 Id TKO cochleae, although OHC differentiation was inhibited and the total number of hair cells per unit length was decreased (Fig. 3K). It is difficult to conclude from these experiments whether Id downregulated Atoh1 expression directly or indirectly due to the decrease of OHCs, but Atoh1 expression was decreased in E16.5 Id TKO cochleae (Fig 7C, D). RNA-Seq analysis using E16.5 control and *Id* TKO cochlear sensory epithelium also showed that Log2 Fold Change of *Atoh1* was -1.142, that is, *Atoh1* expression of *Id* TKO cochlea was approximately half of that of control cochlea.

We next performed an *ex vivo* cochlear culture experiment with Bmp4 and Noggin and analyzed the transcript levels of *Atoh1* in E13.5 cochlear epithelium after culture for 24 h. *Atoh1*

expression in cochlear explants cultured with Bmp4 was not significantly different from *Atoh1* expression in control explants (Fig 7E). *Atoh1* expression was not significantly changed by the application of 1 μg/ml Noggin, while 10 μg/ml Noggin significantly decreased *Atoh1* expression (Fig 7F). *Id1-3* were also decreased by administration of 10 μg/ml Noggin (Fig. S3B). These results indicate that the Bmp4-Id pathway promotes *Atoh1* expression at E13.5 but the effect is not dose-dependent.

Discussion

Id genes are required for the morphogenesis of the cochlear duct

Id genes reportedly regulate not only differentiation but also proliferation in many systems such as the retina (Du et al., 2011), hematopoietic cells (Miyazaki et al., 2015), and the brain (Niola et al., 2012). We also found a catastrophic failure in cochlear morphogenesis of *Id* TKO. This phenotype results from both decreased proliferation and increased cell death.

Redundant functions of *Id* genes have been suggested in brain and heart development. In the developing mouse brain, constitutive deletion of one Id family member does not significantly impact brain development, whereas constitutive *Id1/3*-knockout mice exhibit premature differentiation and major defects in the vasculature of the brain that lead to embryonic lethality between E10.5 and E13.5 (Lyden et al., 1999). Deleting three out of the four *Id* genes (*Id1,2,3* triple gene knockout) caused complex cardiac defects but did not ablate the heart in these embryos, whereas CRISPR/Cas9-mediated deletion of all four *Id* family members in mouse embryos blocked early cardiac progenitor formation and yielded embryos without a heart (Cunningham et al., 2017). These reports imply that *Id* family members have redundant and compensatory activity. The deletion of all four *Id* family members may result in amorphy of cochlea. Huh et al. showed that the mesenchymal Fgf signals regulate the cochlear length (Huh et al., 2015). Because *Id1* and *Id2* were also deleted in the cochlear mesenchymal cells of *Id* TKO mice, deletion of *Id1* and *Id2* might affect the Fgf signaling pathway in the cochlear mesenchyme and thereby shorten the cochlear duct. Further investigation would be required to clarify the unelucidated parts of *Id* genes function in the morphology formation of cochlear duct.

Id1–3 are downstream effectors of Bmp signaling and may mediate Bmp4 positive feedback

It was previously reported that *Id2* expression is lost in the floor of the cochlear duct of *Alk3/6* type I Bmp receptor mutants, and that *Bmp4* expression is also entirely absent in the lateral non-sensory domain next to the prosensory domain in mutants (Ohyama et al. 2010). It was

suggested that *Bmp4* expression is regulated by positive feedback, although the molecular mechanism was unclear. We found that the *Bmp4*-expressing non-sensory domain was lost in *Id* TKO cochlear epithelium. RNA-Seq analysis of *Id* TKO cochlea also revealed the downregulation of *Bmp4* expression. These data suggested that *Id1–3* function not only as downstream effectors of Bmp4 signaling but also regulate Bmp4 positive feedback. Indeed, we found that *Id1–3* maintain *Bmp4* expression by suppressing *Grem1*, a Bmp antagonist (Fig. S4). In kidney development, *Grem1* reportedly represses *Bmp4* expression, and this interaction is necessary for proper kidney development (Michos et al., 2007). The inhibitory effects of *Grem1* on *Bmp4* expression might be a universal property in organ formation.

Involvement of Ids in Bmp signaling for establishing lateral compartments

Ohyama et al. analyzed the cochlear epithelium of *Alk3/6* type I Bmp receptor compound mutants, and reported that the majority of the cochlear epithelium became a *Jag1*-positive medial non-sensory domain, which lacks p27Kip1-positive prosensory and lateral non-sensory domains (Ohyama et al., 2010). The results indicated that Bmp signaling is necessary for patterning of the sensory and non-sensory domains across the medial-lateral axis. We found that *Id* TKO mutants lost the lateral non-sensory domains expressing *Bmp4* and *Lmo3*. *Id* TKO differed from *Alk3/6* type I Bmp receptor compound mutants in the presence or absence of p27Kip1-positive prosensory domain; *Id* TKO retained p27Kip1-positive prosensory domain as well as the medial non-sensory domain. There are two possible explanations for the phenotypic differences between these mutants. Firstly, the Cre-driver mouse line that we used to produce Id TKO cochleae was different from that Ohyama et al. The Cre-recombinase in $Emx2^{cre/+}$ mice starts functioning at E11.5, and the efficiency of recombination in these mice is approximately 90% at E14.5 (Tateya et al., 2011). In contrast, the Cre-recombinase in $Pax2^{cre/+}$ mice starts functioning as early as E9.5, and the efficiency of recombination in these mice is approximately 90% at E10.5 (Duncan and Fritzsch 2013). Therefore, Cre-driven recombination in $Emx2^{cre/+}$ mice might have occurred too late to establish sensory and non-sensory compartment formation across the medial-lateral axis. It may also account for the presence of Sox2-positive cells and Prox1-positive cells in the cochlear explants treated by Bmp inhibitor (Fig 6D, K, L). Secondly, Bmp7 is possibly involved in generating the discrepancy in phenotypes observed between the triple KO and Alk3/6 type I Bmp receptor compound mutants. In any case, Ids are likely to be involved in OHC differentiation mediated by the Bmp-Id signaling pathway.

Bmp-Id signaling promotes the differentiation of OHCs in the organ of Corti

We found that Bmp-Id signaling was necessary for OHC differentiation *in vivo*. Prosensory cells of *Id* TKO cochlea remained undifferentiated state or differentiated into supporting

cells instead of OHCs. We performed an *ex vivo* experiment using cochlear explants, and found that a Bmp inhibitor suppressed OHC differentiation in the cochlear explants prepared from E13.5 embryos. It is suggested that Bmp-Id signaling not only organizes the lateral non-sensory compartment but also promotes OHC differentiation.

There was a discrepancy between *Id* TKO cochlea and cochlear explants cultured with a Bmp inhibitor. Two rows of $p75^{NTR}$-positive cells observed in *Id* TKO cochlea did not occur in cochlear explants cultured with a Bmp inhibitor. Two rows of $p75^{NTR}$-positive cells indicated the incomplete disturbance of the medial-lateral axis formation. Sensory and non-sensory compartment formation across the medial-lateral axis might be determined earlier than E13.5, when the cochlear explants were prepared. Previous studies implied the possibility that the size and boundary of the sensory and non-sensory compartments are affected by Wnt and Bmp signaling before E13.5 (Ohyama et al., 2010; Munnamalai and Fekete., 2016). Another possibility is that the inhibitory effect of *Id* TKO on Bmp signaling is stronger than that of LDN193189. Recombinase efficiency in $Emx2^{cre/+}$ mice is approximately 90% at E14.5 (Tateya et al., 2011), whereas *Id1–3* and *Bmp4* expression was downregulated by ~80% when explants were cultured with 400nM LDN193189 for 24 h.

Noggin (a Bmp antagonist) knockout mice have increased the number of OHC rows (Hwang et al., 2010), suggesting that augmentation of Bmp signaling during cochlear development results in increased rows of OHCs. The exogenous application of Bmp4 to cochlear explants at E15.5 significantly increases the number of OHCs (Puligilla et al., 2007). Conversely, OHC differentiation was inhibited in cochlear explants treated with dorsomorphin (a Bmp signaling inhibitor) from E13.5 or E15.5 to E18.5 (Munnamalai and Fekete., 2016), as treated with LDN193189. These studies together emphasize the opposing roles of Bmp signaling in OHC differentiation. Similarly, progenitor cells, in which the expression of *Id* genes was maintained during hair cell differentiation, were reported to be inhibited from developing as hair cells, indicating a key role for *Id* genes in the negative regulation of expression of *Atoh1* and hair cell differentiation in the developing cochlea (Jones et al., 2006). The results of this study appeared to conflict with our results. However, it seems that the roles of *Id* genes depend on the periods of cochlear development; Ids function to establish the medial-lateral axis of cochlea duct in the pre-prosensory periods, to promote OHC differentiation through Bmp signaling in the prosensory period, and to inhibit Atoh1 activity as antagonists of bHLH in the differentiation period. Jones et al. proposed the working model for the role of Ids in the development of the organ of Corti (Jones et al., 2006); Initially, *Ids* are expressed throughout the prosensory cells that will develop as either hair cells or supporting cells. As development continues, the same cells begin to express *Atoh1*, indicating that Ids are not capable of completely inhibiting *Atoh1* expression. However, in cells that express both Ids and Atoh1, Atoh1 appears incapable of upregulating its own transcription to a level sufficient to activate the downstream signaling pathway that is required for hair cell formation. It appears that, initially, there

is a balance of expression levels between *Id* and *Atoh1*; however, as time progresses, *Id* expression is downregulated in some cells, leading to increased Atoh1 activity and a commitment toward the hair cell fate. In contrast, in cells that maintain *Id* expression, Atoh1 activity continues to be inhibited. We would like to add new insights to this model; Atoh1 may not be the only factor antagonized by Ids, and Ids regulate cochlear morphogenesis and the medial-lateral axis formation before *Atoh1* expression in the cochlear epithelium.

Materials and Methods

Mice

Id1 knockout (Perry et.al., 2007) and *Id3* floxed mice (Guo et. al. 2011) were obtained from Jackson Laboratory. *Id2* knockout mice (Yokota et. al. 2011) were obtained from Dr. Manabu Sugai (University of Fukui School of Medical Sciences, Fukui Japan). *Id1* knockout, *Id2* knockout, *Id3* floxed mice, and $Emx2^{cre/+}$ mice (Kimura et al., 2005) were used to produce various compound heterozygous or homozygous mutant mice. Id1 ; Id2 heterozygous ($Id1^{-/+}$; $Id2^{-/+}$), and Id1 homozygous ($Id1^{-/-}$) mutant mice were used as experimental controls. These mice were maintained on a C57BL/6; ICR mixed background. The date of the appearance of the vaginal plug was defined as E0.5. The mice were genotyped by PCR.

Histochemistry and in situ hybridization

Whole heads (E11.5–16.5) or inner ears (E16.5–18.5) were fixed immediately in 4% paraformaldehyde in phosphate-buffered saline (PBS), cryoprotected in 30% sucrose in PBS, and embedded in OCT for cryostat sectioning. For whole mount immunofluorescence, cochleae were isolated and fixed in 4% paraformaldehyde. The samples were washed with PBS and blocked with PBS containing 0.1% Triton X-100 and 0.5% donkey serum. The following primary antibodies were used: anti-myosin VI (1:200; Proteus), anti-SOX2 (1:200; Millipore), anti-p75 (1:200; Covance), anti-$p27^{kip1}$ (1:200; BD Transduction Laboratories), anti-myosin VIIA (1:200; Developmental Studies Hybridoma Bank), anti-Prox1 (1:200; Merck Millipore) and anti-E-cadherin (1:200; TAKARA). Donkey anti-species IgG conjugated with Alexa 488 or Alexa 594 were used as secondary antibodies. Actin filaments were stained with Alexa488-conjugated phalloidin (1:200; Invitrogen-Molecular Probes). Apoptotic cells were detected using anti-Cleaved Caspase-3 antibody (1:200; Cell signaling technology). Nuclei were stained with 4,6′-diamidino-2-phenylindole (DAPI). For $p27^{kip1}$ and Prox1 staining, sections were heated in 10mM sodium citrate at 90°C for 10 min prior to the addition of the primary antibodies (Tateya et al., 2011). For staining whole mount preparations of the cochlea, cochlear ducts were opened to expose the developing sensory epithelium prior to staining (Yamamoto et al., 2009). *In situ* hybridization was performed using mouse Id1, Id2, Id3, Id4, Bmp4, Fgf10, Fgf8, Jag1, LMO3, LMO4, Lmx1a and Atoh1 probes, as described previously (Imayoshi et al., 2008).

RT-qPCR

Cochlear epithelium was isolated from cultured cochlear explants using thermolysin treatment. An RNeasy Micro Kit (QIAGEN) was used to isolate total RNA, which was reverse-transcribed using ReverTra Ace (TOYOBO) and random primers (TOYOBO). qPCR was performed

with a SYBR Green Kit (Invitrogen) and gene-specific primer sets on a StepOne Plus PCR Detection System (Applied Biosystems/Invitrogen). *GAPDH* was used as a control. The following primers were used for qPCR: *GAPDH* forward, AAT GTG TCC GTC GTG GAT CTG A; *GAPDH* reverse, AGT GTA GCC CAA GAT GCC CTT C; *Id1* forward, TGG GCA CCA GCT CCT TGA; *Id1* reverse, GAA CGT CCT GCT CTA CGA CAT G; *Id2* forward, CAC CAG AGA CCT GGA CAG AA; *Id2* reverse, CAA GGA CAG GAT GCT GAT GT; *Id3* forward, AGA CTA CAT CCT CGA CCT TCA G; *Id3* reverse, AAA AGC TCC TCT TGT CCT TGG; *Bmp4* forward, AGC CCG CTT CTG CAG GA; *Bmp4* reverse, AAA GGC TCA GAG AAG CTG CG; *Atoh1* forward, ATGCACGGGCTGAACCA; *Atoh1* reverse, TCGTTGTTGAAGGACGGGATA; *Hey1* forward, CGGACGAGAATGGAAACTTGA; *Hey1* reverse, CCAAAACCTGGGACGATGTC; *Hey2* forward, AAGCGCCCTTGTGAGGAAA; and *Hey2* reverse, TCGCTCCCCACGTCGAT.

Organ culture

E13.5 mice were used for organ culture. The cochlear epithelium with the surrounding mesenchyme and spiral ganglion neurons was cultured in a culture insert (Millipore) in DMEM/F-12 supplemented with 3 mg/mL glucose and 0.1 mg/mL ampicillin (Ono et al., 2009). For RT-qPCR, cochlear epithelium isolated from the surrounding mesenchyme treated with thermolysin was cultured with the drug to be assessed. Bmp4 was used at a concentration of 50 or 100 ng/mL; Noggin was used at a concentration of 10 μg/mL; and LDN193189 was used at a concentration of 400nM.

RNA-Seq and transcriptome analysis of E16.5 Id TKO cochlear duct

We collected control and *Id* TKO cochlear epithelium without mesenchyme treated with thermolysin at E16.5. We extracted 150–300 ng RNA using an RNeasy Micro Kit (QIAGEN). The RNA integrity number of the samples was 10. Dnaform, Inc. performed sample preparation and sequencing at their facility. The total RNA samples were converted into a cDNA library using a SMARTer Stranded Total RNA Sample Prep Kit. Individually barcoded 50bp+25bp paired-end library products were sequenced on NextSeq500, yielding 36–49 million pair reads. DNA read quality was evaluated in fastq format using FastQC. Adapters, polyA, and polyT sequences were trimmed. The trimmed reads were mapped to the *Mus musculus* genome using STAR40. Read counts for each gene were calculated using featureCounts. Differential expression was evaluated using DESeq2. The cutoff for significantly differentially expressed genes was a false discovery rate-adjusted p-value < 0.05. GO analysis was carried out using clusterprofiler. Pathway analysis was evaluated using Ingenuity Pathway Analysis.

Statistical analysis

Three or more mice from each group were analyzed in all experiments, except RNA-Seq, in which two mice were used. Data are expressed as the mean ± standard error. Student-Newman-Keuls tests were used to detect differences among groups. Differences at $p < 0.05$ were regarded as statistically significant.

Quantification of proliferation in the prosensory domain

To analyze the proliferation of the cochlear epithelium, pregnant female mice were injected with 50 μg/body weight EdU. Embryos were obtained at 2 h after EdU injection. Surface preparations of E12.5 control and *Id* TKO mice cochleae were immunolabeled for Sox and EdU. EdU was detected with a Click-it EdU Alexa Fluor 594 Imaging Kit (Invitrogen). EdU-positive cells in 27000 μm^3 Sox2-positive cochlear epithelium at the basal turn were counted using Zen. Counting was normalized to 1000μm^3 Sox2-positive cochlear epithelium.

Measurement of cochlear length

Cochleae were dissected from embryos at E18.5. Cochlear surface preparations of various *Id* compound mutants were stained with phalloidin and myosin VI. The entire length of the cochlea was measured using LSM510 operating software (Tateya et al., 2013).

Quantification of hair cells

The number of hair cells was counted using whole-mounted E18.5 cochleae processed with MyosinVIIA immunohistochemistry. Hair cells were regarded as the cells inside the row visualized by $p75^{NTR}$ immunostaining. We analyzed basal half of each cochlea.

Acknowledgments

We thank Dr. Shinichi Aizawa for the Emx2$^{cre/+}$ mice and Dr. Manabu Sugai for the Id2$^{-/-}$ mice. This work was supported by Core Research for Evolutional Science and Technology (CREST) (JPMJCR12W2, R.K.), Grant-in-Aid for Scientific Research on Innovative Areas (16H06480, R.K.) and (25462635, T.T.) from Ministry of Education, Culture, Sports, Science, and Technology (MEXT), Japan.

Competing interests statement:

The authors declare no competing financial interests.

Author contributions:

S.S., T.T., K.O. and R.K. designed the project and wrote the manuscript.

S.S. and T.T. performed mouse breeding and all experiments.

References

Benito-Gonzalez A and Doetzlhofer A. Hey1 and Hey2 Control the Spatial and Temporal Pattern of Mammalian Auditory Hair Cell Differentiation Downstream of Hedgehog Signaling. J Neurosci. 2014 Sep 17;34(38):12865-76.

Bermingham-McDonogh O, Oesterle EC, Stone JS, Hume CR, Huynh HM, Hayashi T. Expression of Prox1 during mouse cochlear development. J Comp Neurol. 2006; 496(2):172-86.

Chang W., Lin, Z., Kulessa, H., Hebert, J., Hogan, B. L. M. and Wu. D.K. (2008). Bmp4 is essential for the formation of the vestibular apparatus that detects angular head movements. PLoS Genet 4, e1000050.

Chang W, Lin Z, Kulessa H, Hebert J, Hogan BL, Wu DK. Bmp4 is essential for the formation of the vestibular apparatus that detects angular head movements. PLoS Genet. 2008 ;4(4):e1000050. doi: 10.1371/journal.pgen.1000050.

Chen YS, Aubee J, DiVito KA, Zhou H, Zhang W, Chou FP, Simbulan-Rosenthal CM, Rosenthal DS. Id3 induces an Elk-1-caspase-8-dependent apoptotic pathway in squamous carcinoma cells. Cancer Med. 2015 ;4(6):914-24. doi: 10.1002/cam4.427.

Chizhikov VV, Millen KJ. Control of roof plate development and signaling by Lmx1b in the caudal vertebrate CNS. J Neurosci. 2004;24(25):5694-703.

Cunningham TJ, Yu M., McKeithan W., Spiering S, Carrette F, Huang CT, et al. Id genes are essential for early heart formation. Genes Dev. 2017;31(13):1325-1338. doi: 10.1101/gad.300400.117.

Dabdoub A, Puligilla C, Jones JM, Fritzsch B, Cheah KS, Pevny LH, et al. Sox2 signaling in prosensory domain specification and subsequent hair cell differentiation in the developing cochlea. Proc Natl Acad Sci U S A. 2008;105(47):18396-401. doi: 10.1073/pnas.0808175105.

de la Calle-Mustienes E, Lu Z, Cortés M, Andersen B, Modolell J, Gómez-Skarmeta JL. *Xenopus Xlmo4* is a GATA cofactor during ventral mesoderm formation and regulates Ldb1 availability at the dorsal mesoderm and the neural plate. Dev Biol. 2003 Dec 15;264(2):564-81.

Deng M, Luo XJ, Pan L, Yang H, Xie X, Liang G, et al. LMO4 functions as a negative regulator of sensory organ formation in the mammalian cochlea. J Neurosci. 2014 Jul 23;34(30):10072-7. doi: 10.1523/JNEUROSCI.0352-14.2014.

Du Y, Yip HK. The expression and roles of inhibitor of DNA binding helix-loop-helix proteins in the developing and adult mouse retina. Neuroscience. 2011;175:367-79. doi: 10.1016/j.neuroscience.2010.12.007.

Duncan JS, and Fritzsch B. Continued expression of GATA3 is necessary for cochlear neurosensory development. PLoS One. 2013;8(4):e62046. doi: 10.1371/journal.pone.0062046.

Groves AK, Fekete DM. Shaping sound in space: the regulation of inner ear patterning. Development. 2012;139(2):245-57. doi: 10.1242/dev.067074.

Groves AK, Zhang KD, Fekete DM. The genetics of hair cell development and regeneration. Annu Rev Neurosci. 2013;36:361-81. doi: 10.1146/annurev-neuro-062012-170309.

Guo Z, Li H, Han M, Xu T, Wu X, Zhuang Y. Modeling Sjögren's syndrome with Id3 conditional knockout mice. Immunol Lett. 2011 Mar 30;135(1-2):34-42. doi: 10.1016/j.imlet.2010.09.009.

Hollnagel A, Oehlmann V, Heymer J, Rüther U, Nordheim A. Id genes are direct targets of bone morphogenetic protein induction in embryonic stem cells. J Biol Chem. 1999;274(28):19838–19845.

Huh SH, Warchol ME and Ornitz DM. Cochlear progenitor number is controlled through mesenchymal FGF receptor signaling. Elife. 2015 Apr 27;4.

Huang M, Sage C, Li H, Xiang M, Heller S, Chen ZY. Diverse expression patterns of LIM-homeodomain transcription factors (LIM-HDs) in mammalian inner ear development. Dev Dyn. 2008;237(11):3305-12. doi: 10.1002/dvdy.21735.

Hwang CH, Guo D, Harris MA, Howard O, Mishina Y, Gan L, et al. Role of bone morphogenetic proteins on cochlear hair cell formation: Analyses of Noggin and Bmp2 mutant mice. Dev Dyn. 2010;239(2):505-13. doi: 10.1002/dvdy.22200.

Imayoshi I, Shimogori T, Ohtsuka T, Kageyama R. Hes genes and neurogenin regulate non-neural versus neural fate specification in the dorsal telencephalic midline. Development. 2008; 135(15):2531-41. doi: 10.1242/dev.021535.

Jones JM, Montcouquiol M, Dabdoub A, Woods C, Kelley MW. Inhibitors of differentiation and DNA binding (Ids) regulate Math1 and hair cell formation during the development of the organ of Corti. J Neurosci. 2006 ;26(2):550-8.

Kamaid A, Neves J, Giráldez F. *Id* gene regulation and function in the prosensory domains of the chicken inner ear: A link between Bmp signaling and *Atoh1*. J Neurosci. 2010 ;30(34):11426-34. doi: 10.1523/JNEUROSCI.2570-10.2010.

Kelley MW. Cellular commitment and differentiation in the organ of Corti. Int J Dev Biol. 2007;51(6-7):571-83.

Kiernan AE, Pelling AL, Leung KK, Tang AS, Bell DM, Tease C, et al. *Sox2* is required for sensory organ development in the mammalian inner ear. Nature. 2005;434(7036):1031-5.

Kimura J, Suda Y, Kurokawa D, Hossain ZM, Nakamura M, Takahashi M, et al. *Emx2* and *Pax6* function in Cooperation with *Otx2* and *Otx1* to develop caudal forebrain primordium that includes future archipallium. J Neurosci. 2005 ;25(21):5097-108.

Korchynskyi O, ten Dijke P. Identification and functional characterization of distinct critically important bone morphogenetic protein-specific response elements in the Id1 promoter. J Biol Chem. 2002;277(7):4883–4891.

Lasorella A, Noseda M, Beyna M, Yokota Y, Iavarone A. Id2 is a retinoblastoma protein target and mediates signalling by Myc oncoproteins. Nature. 2000 Oct 5;407(6804):592-8.

Le Dréau G, Escalona R, Fueyo R, Herrera A, Martínez JD, Usieto S, et al. E proteins sharpen neurogenesis by modulating proneural bHLH transcription factors' activity in an E-box-dependent manner. Elife. 2018;7. pii: e37267. doi: 10.7554/eLife.37267.

Lee TK, Man K, Ling MT, Wang XH, Wong YC, Lo CM, Poon RT, et al. Over-expression of Id-1 induces cell proliferation in hepatocellular carcinoma through inactivation of p16INK4a/RB pathway. Carcinogenesis. 2003 Nov;24(11):1729-36.

Lyden D, Young AZ, Zagzag D, Yan W, Gerald W, O'Reilly R, et al. Id1 and Id3 are required for neurogenesis, angiogenesis and vascularization of tumour xenografts. Nature. 1999;401(6754):670-7.

López-Rovira T, Chalaux E, Massagué J, Rosa JL, Ventura F. Direct binding of Smad1 and Smad4 to two distinct motifs mediates bone morphogenetic protein-specific transcriptional activation of Id1 gene. J Biol Chem. 2002;277(5):3176–3185.

Mann ZF, Gálvez H, Pedreno D, Chen Z, Chrysostomou E, Żak M, et al. Shaping of inner ear sensory organs through antagonistic interactions between Notch signalling and Lmx1a. Elife. 2017 ;6. pii: e33323. doi: 10.7554/eLife.33323.

Michos O, Gonçalves A, Lopez-Rios J, Tiecke E, Naillat F, Beier K, et al. Reduction of BMP4 activity by gremlin 1 enables ureteric bud outgrowth and GDNF/WNT11 feedback signalling during kidney branching morphogenesis. Development. 2007;134(13):2397-405.

Miyazaki M, Miyazaki K, Chen S, Chandra V, Wagatsuma K, Agata Y, et al. The E-Id protein axis modulates the activities of the PI3K-AKT-mTORC1-Hif1a and c-myc/p19Arf pathways to suppress innate variant TFH cell development, thymocyte expansion, and lymphomagenesis. Genes

Dev. 2015 ;29(4):409-25. doi: 10.1101/gad.255331.114.

Morsli H, Choo D, Ryan A, Johnson R, Wu DK. Development of the mouse inner ear and origin of its sensory organs. J Neurosci. 1998;18(9):3327-35.

Munnamalai V. Fekete DM. Notch-Wnt-Bmp crosstalk regulates radial patterning in the mouse cochlea in a spatiotemporal manner. Development. 2016;143(21):4003-4015.

Niola F1, Zhao X, Singh D, Castano A, Sullivan R, Lauria M, et al. Id proteins synchronize stemness and anchorage to the niche of neural stem cells. Nat Cell Biol. 2012;14(5):477-87. doi: 10.1038/ncb2490.

Ohyama T, Basch ML, Mishina Y, Lyons KM, Segil N, Groves AK. BMP signaling is necessary for patterning the sensory and nonsensory regions of the developing mammalian cochlea. J Neurosci. 2010 Nov 10;30(45):15044-51. doi: 10.1523/JNEUROSCI.3547-10.2010.

Ono K1, Nakagawa T, Kojima K, Matsumoto M, Kawauchi T, Hoshino M, et al. Silencing p27 reverses post-mitotic state of supporting cells in neonatal mouse cochleae. Mol Cell Neurosci. 2009;42(4):391-8. doi: 10.1016/j.mcn.2009.08.011.

Ouyang XS, Wang X, Ling MT, Wong HL, Tsao SW, Wong YC. Id-1 stimulates serum independent prostate cancer cell proliferation through inactivation of p16(INK4a)/pRB pathway. Carcinogenesis. 2002;23(5):721-5.

Peng Y, Kang Q, Luo Q, Jiang W, Si W, Liu BA, et al. Inhibitor of DNA binding/differentiation Helix-Loop-Helix proteins mediate bone morphogenetic protein-induced osteoblast differentiation of mesenchymal stem cells. J Biol Chem. 2004;279(31):32941-9.

Perry SS, Zhao Y, Nie L, Cochrane SW, Huang Z, Sun XH. Id1, but not Id3, directs long-term repopulating hematopoietic stem-cell maintenance. Blood. 2007;110(7):2351-60.

Puligilla C, Feng F, Ishikawa K, Bertuzzi S, Dabdoub A, Griffith AJ, et al. Disruption of fibroblast growth factor receptor 3 signaling results in defects in cellular differentiation, neuronal patterning, and hearing impairment. Dev Dyn. 2007;236(7):1905-17.

Roberts EC, Deed RW, Inoue T, Norton JD, Sharrocks AD. Id helix-loop-helix proteins antagonize pax transcription factor activity by inhibiting DNA binding. Mol Cell Biol. 2001 Jan;21(2):524-33.

Samanta J and Kessler JA. Interactions between ID and OLIG proteins mediate the inhibitory effects of BMP4 on oligodendroglial differentiation. Development. 2004;131(17):4131-42.

Simonneau L, Gallego M, Pujol R. Comparative expression patterns of T-, N-, E-cadherins, beta-catenin, and polysialic acid neural cell adhesion molecule in rat cochlea during development: implications for the nature of Kölliker's organ. J Comp Neurol. 2003;459(2):113-26.

Tateya T, Imayoshi I, Tateya I, Ito J, Kageyama R. Cooperative functions of *Hes*/*Hey* genes in auditory hair cell and supporting cell development. Dev Biol. 2011;352(2):329-40. doi: 10.1016/j.ydbio.2011.01.038. PMID: 21300049

Tateya T, Imayoshi I, Tateya I, Hamaguchi K, Torii H, Ito J, et al. Hedgehog signaling regulates prosensory cell properties during the basal-to-apical wave of hair cell differentiation in the mammalian cochlea. Development. 2013;140(18):3848-57. doi: 10.1242/dev.095398. PMID: 23946445

Viñals F, Reiriz J, Ambrosio S, Bartrons R, Rosa JL, Ventura F. BMP-2 decreases Mash1 stability by increasing Id1 expression. EMBO J. 2004;23(17):3527-37. PMID: 15318167

Yamamoto N, Okano T, Ma X, Adelstein RS, Kelley MW. Myosin II regulates extension, growth and patterning in the mammalian cochlear duct. Development. 2009 Jun;136(12):1977-86. doi: 10.1242/dev.030718. PMID: 19439495

Yan W, Young AZ, Soares VC, Kelley R, Benezra R, Zhuang Y. High incidence of T-cell tumors in E2A-null mice and E2A/Id1 double-knockout mice. Mol Cell Biol. 1997;17(12):7317-27.

Yates PR, Atherton GT, Deed RW, Norton JD. Sharrocks AD. Id helix-loop-helix proteins inhibit nucleoprotein complex formation by the TCF ETS-domain transcription factors. EMBO J. 1999 ;18:968–976.

Yokota Y, Mansouri A, Mori S, Sugawara S, Adachi S, Nishikawa S, et al. Development of peripheral lymphoid organs and natural killer cells depends on the helix-loop-helix inhibitor Id2. Nature. 1999;397(6721):702-6. PMID: 10067894

Zúñiga A, Haramis AP, McMahon AP, Zeller,R. Signal relay by BMP antagonism controls the SHH/FGF4 feedback loop in vertebrate limb buds. Nature. 1999;401(6753):598-602. PMID: 10524628

Figure legends

Fig. 1. Expression patterns of *Id1*, *Id2*, *Id3*, and *Id4* during cochlear prosensory domain formation.

(A–N) E12.5 and E13.5 cochlear sections. Immunohistochemistry for Sox2 (green) and DAPI (blue) (A) and Sox2 (green) and $p27^{kip1}$ (magenta) (H). *In situ* hybridization for *Bmp4* (B, I), *Fgf10* (C, J), *Id1* (D, K), *Id2* (E, L), *Id3* (F, M), and *Id4* (G, N). The prosensory domain at E13.5 is indicated by a bracket (H-N). *Id1–3* were expressed in a gradient from the lateral to medial side in the floor of the cochlear duct at E12.5 and E13.5. (O) The schematic images summarize the relative expression patterns of *Id1*, *Id2*, and *Id3* compared with the regional markers *Bmp4*, *Fgf10*, and $p27^{kip1}$. Scale bars, (A) 50 μm, (G) 50 μm for B-G, (H) 50 μm, and (N) 50 μm for I-N.

Fig. 2. *Id1-3* are necessary for adequate cochlear length and morphology.

(A) The surface of various *Id* compound mutant cochlear epithelium by labeling with phalloidin (gray). Scale bar, 100μm. (B) Measurement of cochlear length of *Id* compound mutants. More than three animals were used for each group. Cochlear length was not significantly different between WT, $Id1^{-/-}$, and *Id1Id3* DKO mice. The cochlear length of mutant mice with the $Id2^{-/-}$ allele was significantly shorter than that of WT, *Id1*-/-, and *Id1Id3* DKO mice. The cochlear length of *Id* TKO mice was the shortest among the *Id* compound mutant mice. (C–E) 50μg/body weight EdU was given to pregnant mice at E12.5 by a single intraperitoneal injection at 2 h before sacrifice. Sox2 (green), EdU (red), and DAPI (blue) co-staining of E12.5 control (C,C') and *Id* TKO cochleae (D,D'). Scale bars, 100μm. C' and D' are magnified images of the boxes in C and D, respectively. (E) Quantification of the number of EdU-incorporating cells. (F–I) Control and *Id* TKO cochleae at E12.5 and E14.5 were analyzed for cell death. Whole mount immunostaining for E-cadherin (green) and C-cas3 (magenta) of control (F, F') and *Id* TKO (G, G') at E12.5. F' and G' are cross sections at the dashed lines shown in F and G, respectively. Sections of control (H) and *Id* TKO (I) are immunolabeled with $p27^{kip1}$ (green) and C-cas3 (magenta) at E14.5. Scale bar, 20μm. Arrowheads in G' and I indicate C-cas3-positive apoptotic cells. (J–L, K', L') Cochleae of control (J) and *Id* TKO mice (K-L') were visualized by E-cadherin (green) and Sox2 (magenta). The cochlear duct of *Id* TKO mice was irregular with random expansion and constriction (K, K', L, L'). The Sox2-positive sensory domain of the *Id* TKO cochlear epithelium also had an irregular shape. Arrows indicate regions of expansion. Arrowheads indicate regions of constriction. Scale bar, 50 μm (L, L'). *$p<0.05$, **$p<0.01$, Student t test.

Fig. 3. Decreased numbers of OHCs in *Id* TKO cochlea.

(A–C) Surface of E18.5 control (A) and *Id* TKO cochleae (B, C) by immunolabeling for myosin

VIIA (green) and p75^{NTR} (magenta). Asterisks illustrate p75^{NTR}-positive pillar cells. Sections of E17.5 control (D, D') and *Id* TKO cochleae (E, E', F, F') by labeling for myosin VIIA (green), p75^{NTR} (red), and DAPI (blue). D'–F' are grayscale images of p75^{NTR} staining of D–F. Arrowheads indicate p75^{NTR}-positive pillar cells. Scale bar, 50 μm. (G–J) *Fgf8* expression detected by *in situ* hybridization. Sections of the mid-basal turn of control (G, H) and *Id* TKO (I, J) cochleae are shown. The sections were immunolabeled with myosin VI (magenta) and p27^{kip1} (green). H and J are the same sections as shown in G and I, respectively. Asterisks show *Fgf8*-positive hair cells. (K) The number of hair cells in the organ of Corti. The number of IHCs per 100 μm in *Id* TKO mice was higher than that in control mice. However, the number of OHCs and the total hair cell number per 100 μm was decreased in *Id* TKO mice. $^{**}p<0.01$, Student *t* test. Scale bars, (C) 20 μm for A-C, (F and F') 20 μm for (D–F, D'–F'), (J) 50 μm for G-J.

Fig. 4. Prox1-positive supporting cells are observed lateral to hair cells in *Id* TKO cochlea.

(A–C) Surface preparations of E18.5 control and *Id* TKO cochleae by immunolabeling for myosin VIIA (green) and Prox1 (magenta). Views of the luminal surface (A) and basement membrane (B) of the same control sample are shown. Prox1-positive supporting cells were observed lateral to the hair cells in *Id* TKO cochlea. Sporadically, some hair cells were found in the same region as supporting cells in *Id* TKO cochlea (C). (D–F, D'–F') Sections of E17.5 control and *Id* TKO cochleae visualized by myosin VIIA (green), Prox1 (red), and DAPI (blue). D'–F' are grayscale images of Prox1 staining of the images shown in D–F, respectively. Prox1-positive supporting cells were observed lateral to the hair cells in *Id* TKO cochlea. Scale bars, 20 μm.

Fig. 5. Markers for the future outer sulcus, *Bmp4* and *Lmo3,* are not detected in E16.5 *Id* TKO cochlea.

(A–H) Expression patterns of the GER markers *Fgf10* and *Jag1*, the hair cell marker myosin VI (green), and the prosensory and supporting cell markers p27^{kip1} (magenta) and Sox2 (gray) of control (A-D) and *Id* TKO cochleae (E-H) are shown. One or multiple rows of hair cells were observed in *Id* TKO cochlea. The GER markers *Fgf10* and *Jag1* were detected by *in situ* hybridization in control (B, C) and *Id* TKO (F, G) cochleae. B and F are the same sections as shown in A and E, respectively. (I–M) Markers of the future outer sulcus *Bmp4* and *Lmo3* were detected by *in situ* hybridization in control (I, J) but not in *Id* TKO (K, L) cochlear epithelium. The hair cell marker myosin VI (green) and prosensory and supporting cell marker p27^{kip1} (magenta) of *Id* TKO cochlea are shown (M). L and M show the same section. Scale bars, 50 μm (H and M).

Fig. 6. Effect of inhibiting Bmp signaling on cultured cochlea.

(A) The mRNA levels of *Id1*, *Id2*, *Id3*, and *Bmp4* in E13.5 cochlear explants cultured for 24 h with or without LDN193189 (Bmp4 receptor antagonist) were detected by RT-qPCR. The levels are shown as a ratio to control. The expression levels of *Id1*, *Id2*, *Id3*, and *Bmp4* were downregulated in cochlear explants cultured for 24 h with LDN193189, whereas the expression levels of *Hey1* and *Hey2* did not change. $^{**}p<0.01$, Student *t* test. (B) Schematic images showing the schedule for the age of embryos for cochlear explants, duration of drug treatment, and harvesting. (C, D) Cochlear explants established at E13.5 cultured with (D) or without (C) 400nM LDN193189 for 3 days were visualized by immunostaining for myosin VIIA (green) and Sox2 (magenta). Myosin VIIA-positive OHCs were not detected at the basal turn of cochlear explants cultured with LDN193189. Asterisks indicate IHCs, and brackets indicate OHCs. Scale bar, 20 μm. (E–L) Cochlear explants established at E13.5 cultured with (G,H,K,L) or without (E,F,I,J) 400nM LDN193189 for 3 days were washed and then cultured without LDN193189 for aditional 2 days. The explants were immunolabeled with myosin VIIA (green) and $p75^{NTR}$ (magenta) or with myosin VIIA (green) and Prox1 (magenta). Scale bars, 20 μm.

Fig. 7. Downregulation of *Atoh1* by inhibition of Bmp signaling and in *Id* TKO cochlear epithelium.

(A-D) The expression patterns of *Atoh1* detected by *in situ* hybridization are shown. Representative cross sections of the mid-basal turn at E14.5 and E16.5 in control (A, C) and *Id* TKO (B,D) cochleae are shown. *Atoh1* expression was observed in *Id* TKO cochlea at E14.5 and E16.5. Scale bars, 50 μm. (E) The mRNA levels of *Atoh1* in E13.5 cochlear explants cultured for 6 h with 0 ng/ml (control), 50 ng/ml, 100 ng/ml, or 1μg/ml recombinant Bmp4 (E). The levels detected by RT-qPCR are shown as a ratio to the control. Atoh1 expression in cochlear explants cultured with Bmp4 was not significantly different from Atoh1 expression in control explants. (F) The mRNA levels of *Atoh1* in E13.5 cochlear explants cultured for 6 h with 0μg/ml (control), 1μg/ml or 10 μg/ml recombinant Noggin. The levels detected by RT-qPCR are shown as a ratio to the control. *Atoh1* expression was not significantly changed by the application of 1 μg/ml Noggin, while 10 μg/ml Noggin significantly decreased *Atoh1* expression.

Fig.1

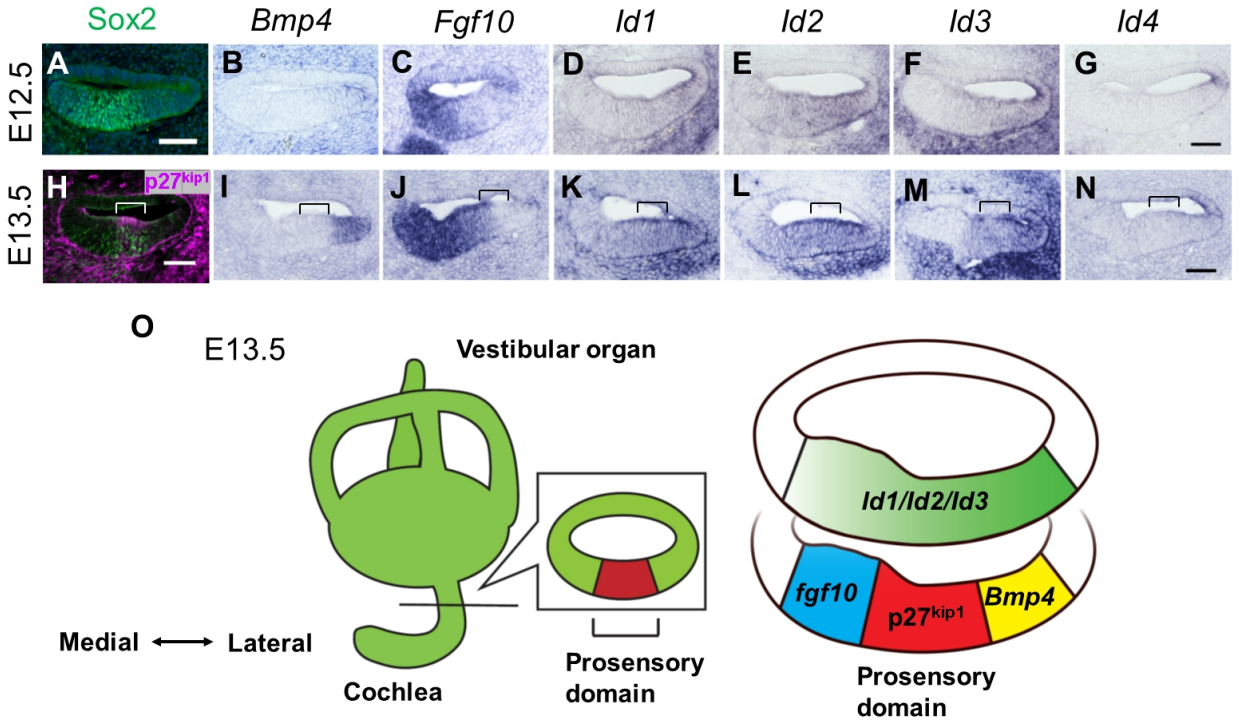
Sox2
Bmp4
Fgf10
Id1
Id2
Id3
Id4
E12.5
E13.5
A
B
C
D
E
F
G
H
p27kip1
I
J
K
L
M
N
O
E13.5
Vestibular organ
Medial
Lateral
Cochlea
Prosensory domain
Id1/Id2/Id3
fgf10
p27kip1
Bmp4
Prosensory domain

E18.5 cochlear length

A

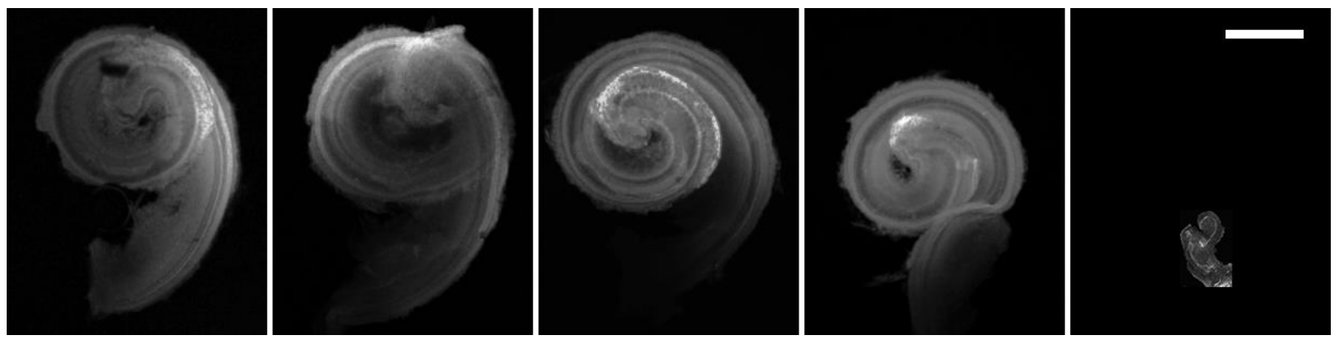

B

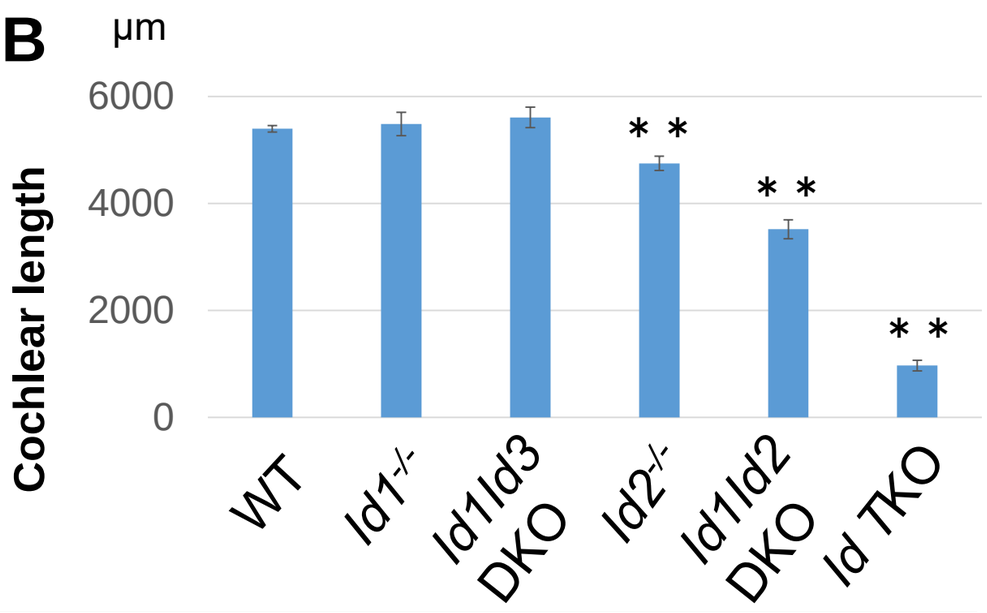

Cell proliferation in E12.5 Sox2-positive prosensory domain

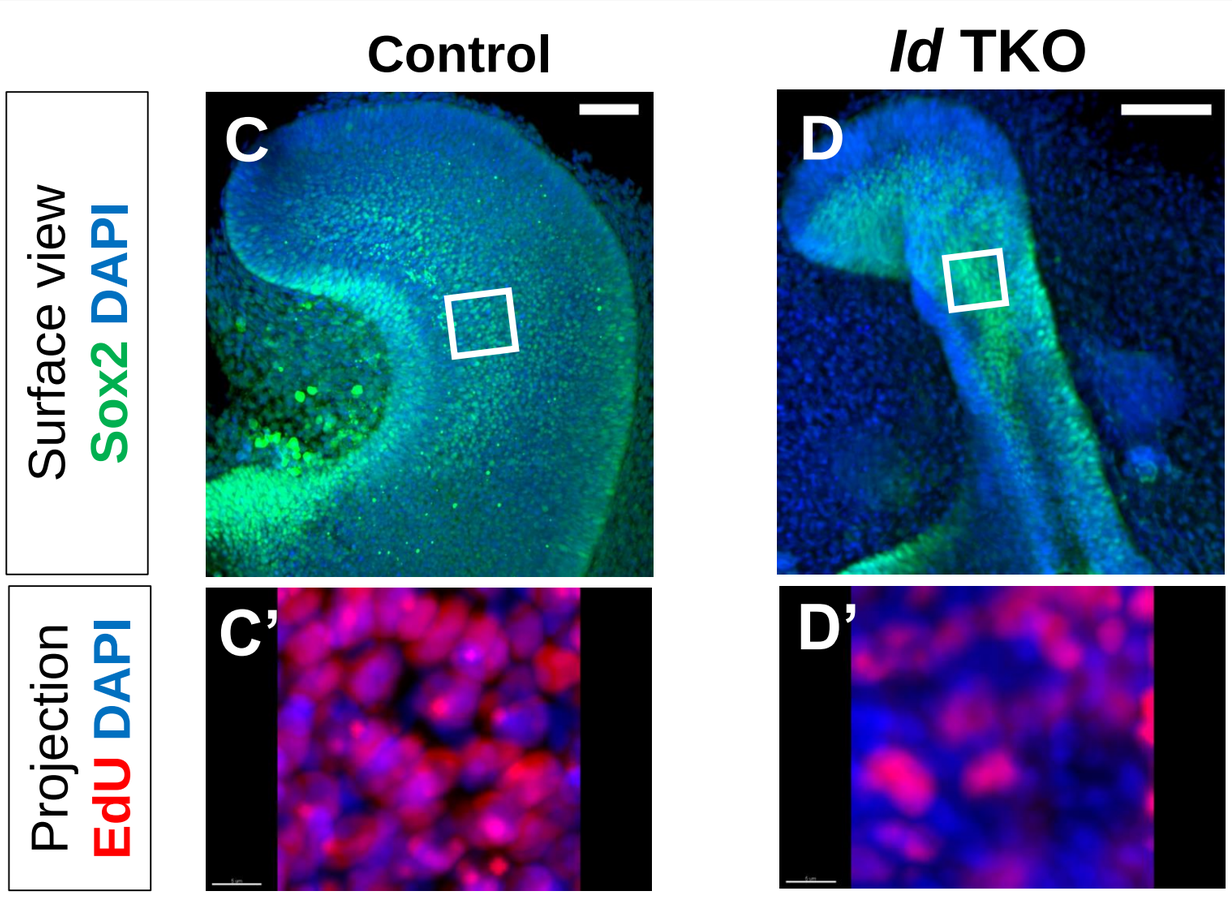

E

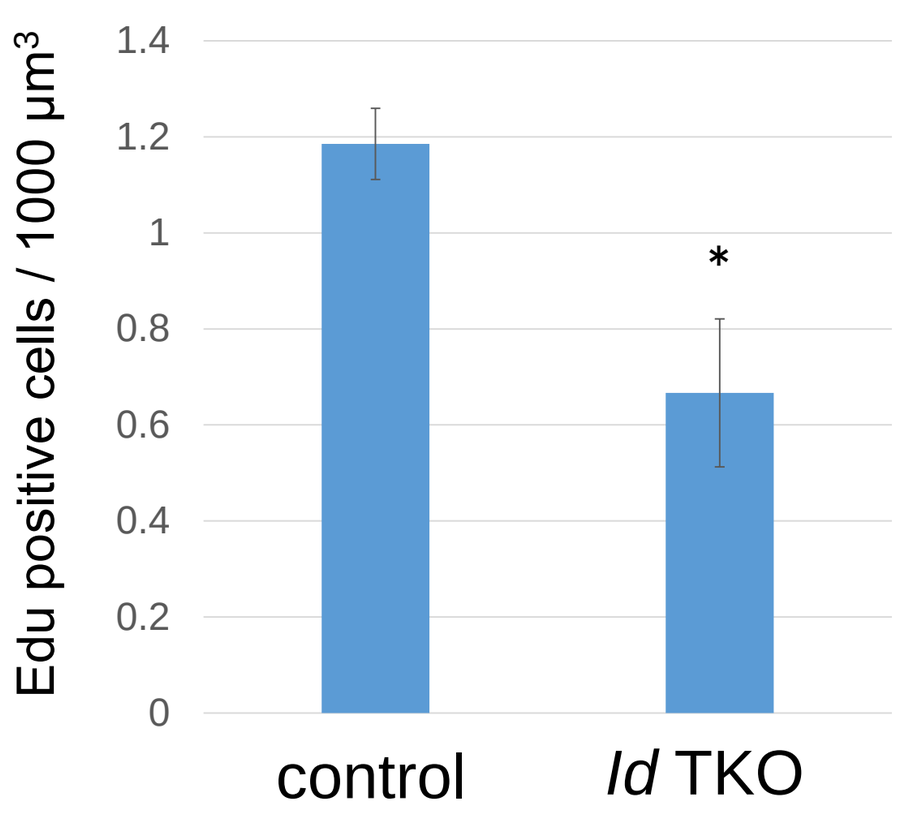

Cell death in cochlear epithelium

E12.5 (C-Cas3 E-Cad)

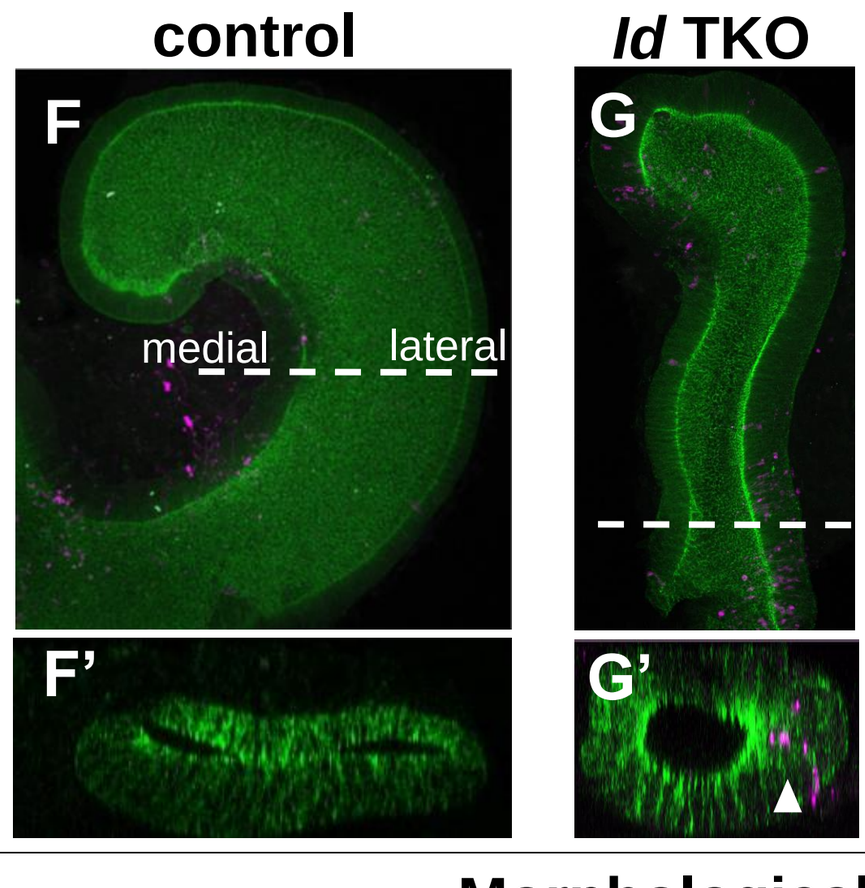

E14.5 (C-Cas3 p27Kip1)

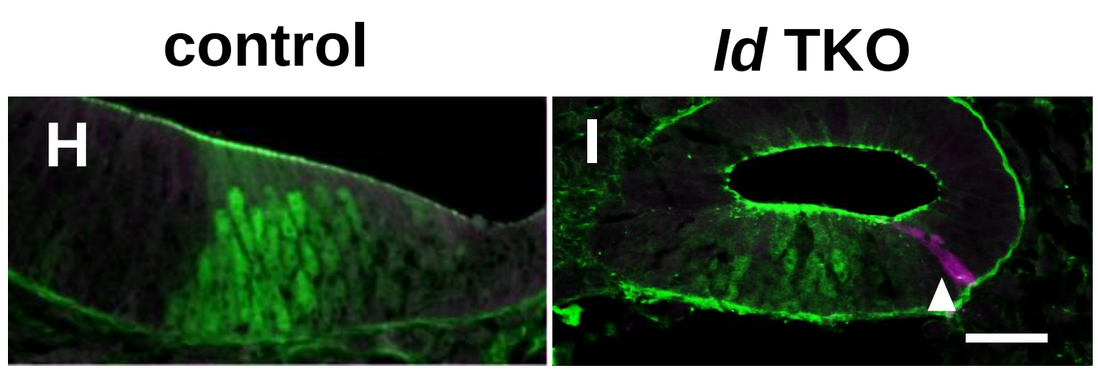

Morphological variation of *Id* TKO

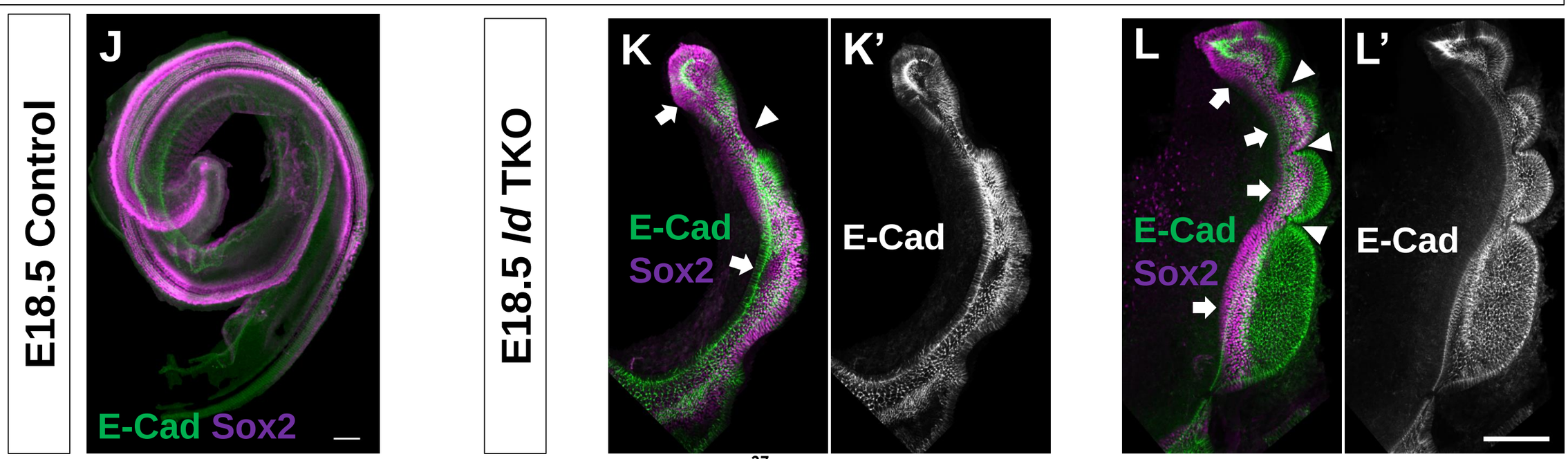

Prox1-positive cell rows of E18.5 cochlear epithelium

E18.5 Control surface view

MyosinVIIA Prox1

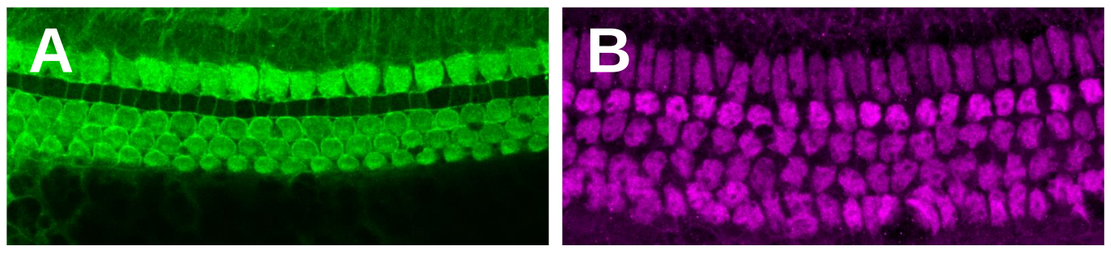

E18.5 *Id* TKO

MyosinVIIA Prox1

Surface view

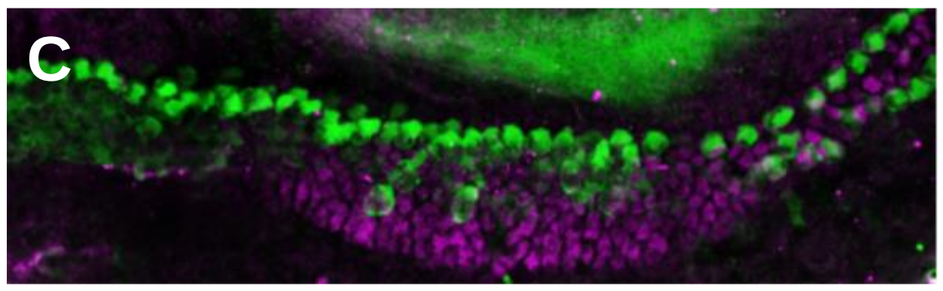

Sectional view

Prox1 MyosinVIIA DAPI

control *Id* TKO

Prox1

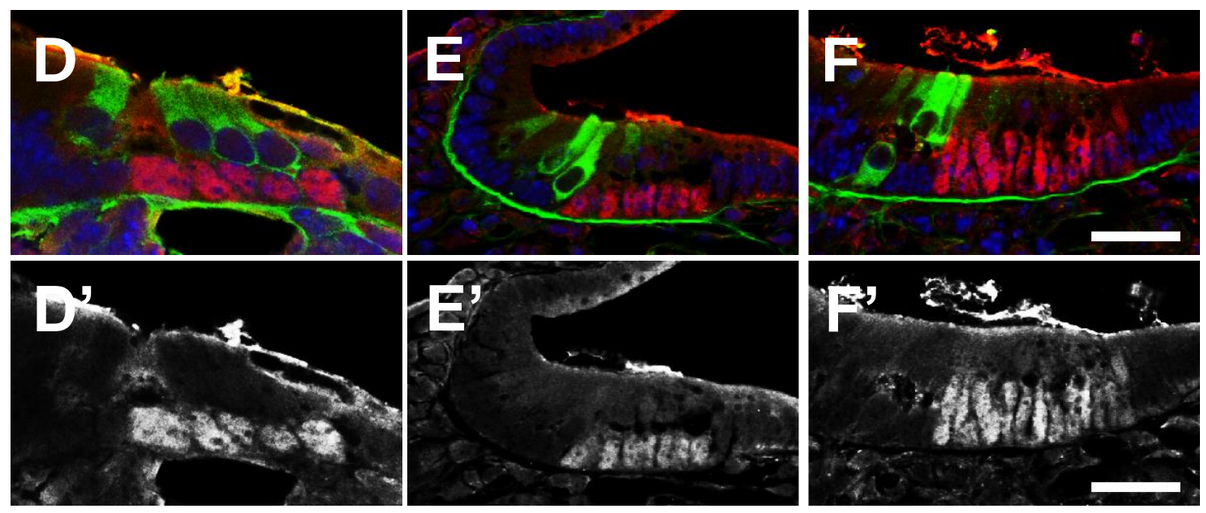

Fig. 3

p75^{NTR}-positive cell rows of cochlear epithelium

Surface view
p75^{NTR} MyosinVIIA

Control

Id TKO

Doublet rows

Single row

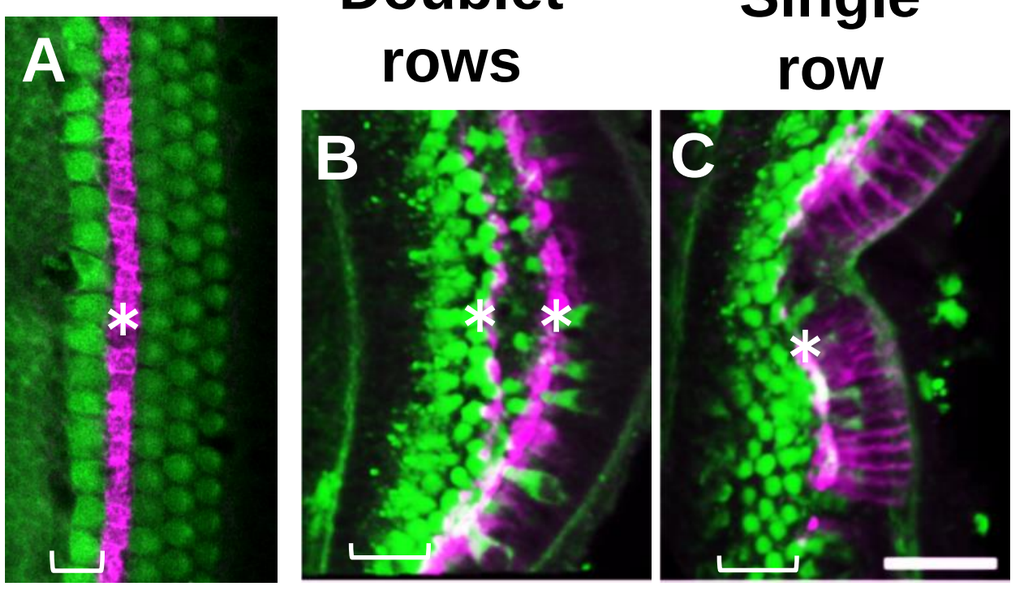

Sectional view
p75^{NTR} Myosin VIIA DAPI

control

Id TKO

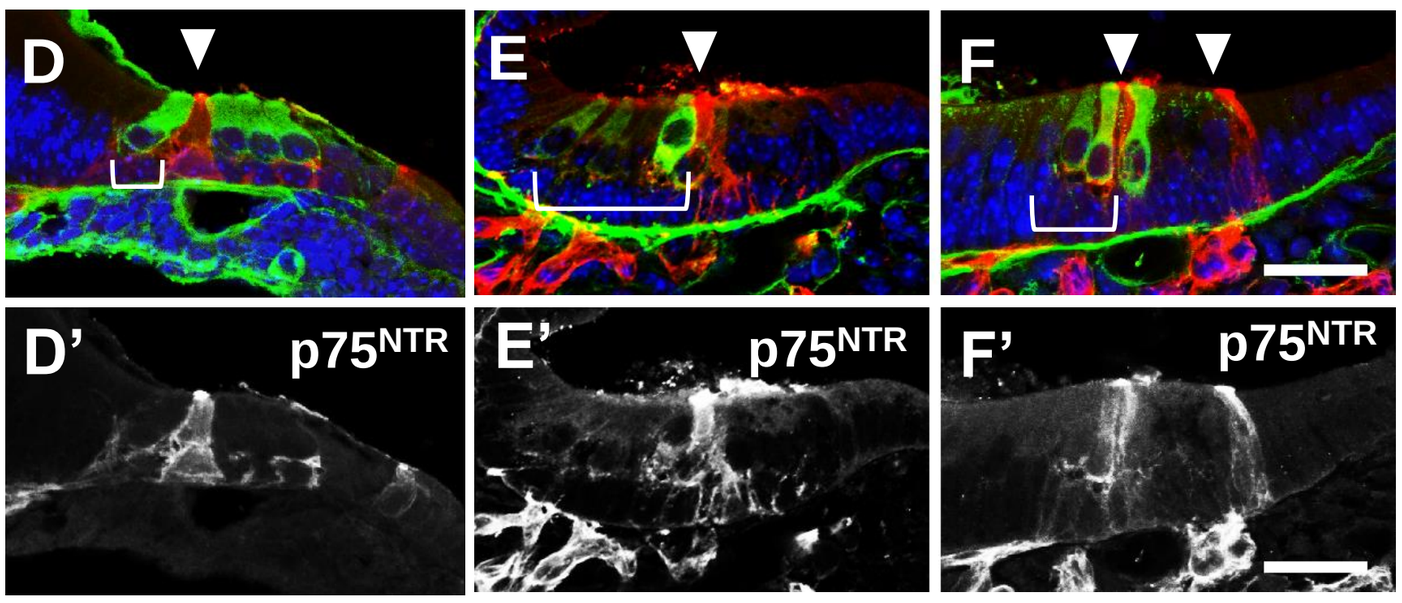

Fgf8 positive inner hair cells

control

Id TKO

Fgf8

p27^{kip1} MyosinVI

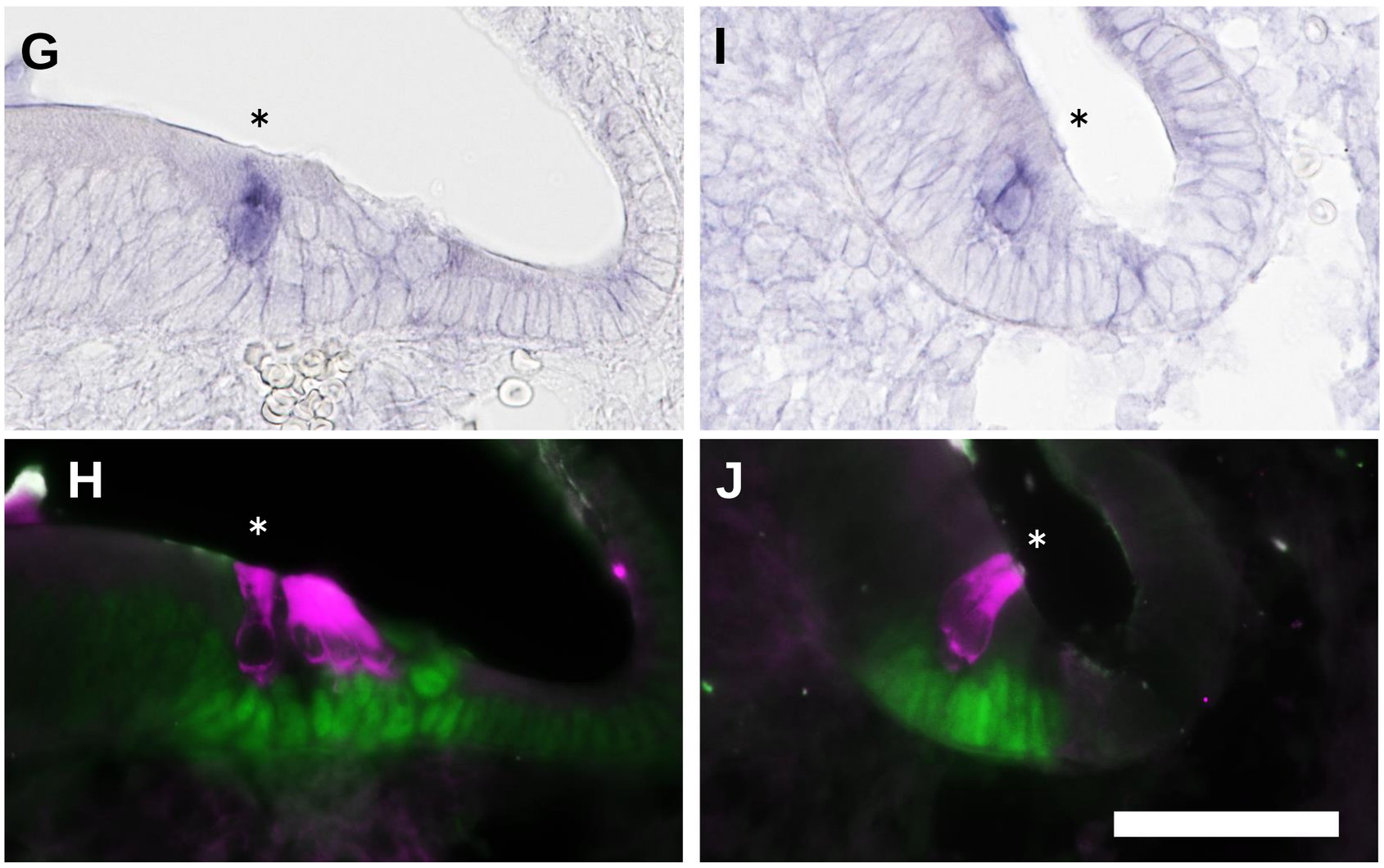

inner hair cell、outer hair cell and total hair cell number of *Id* TKO

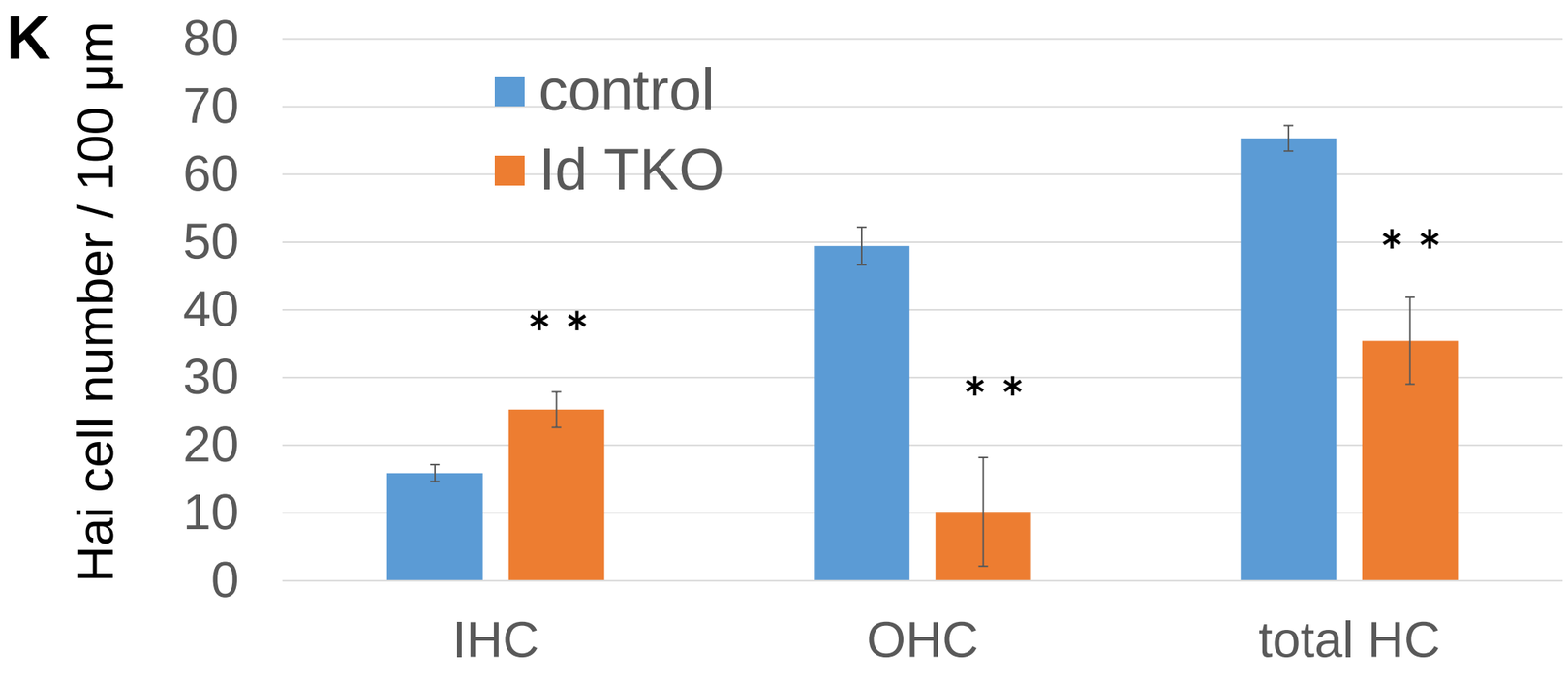

Fig. 5

E16.5 Markers for GER

Control | *Id* TKO

Myosin VI
p27^{Kip1}

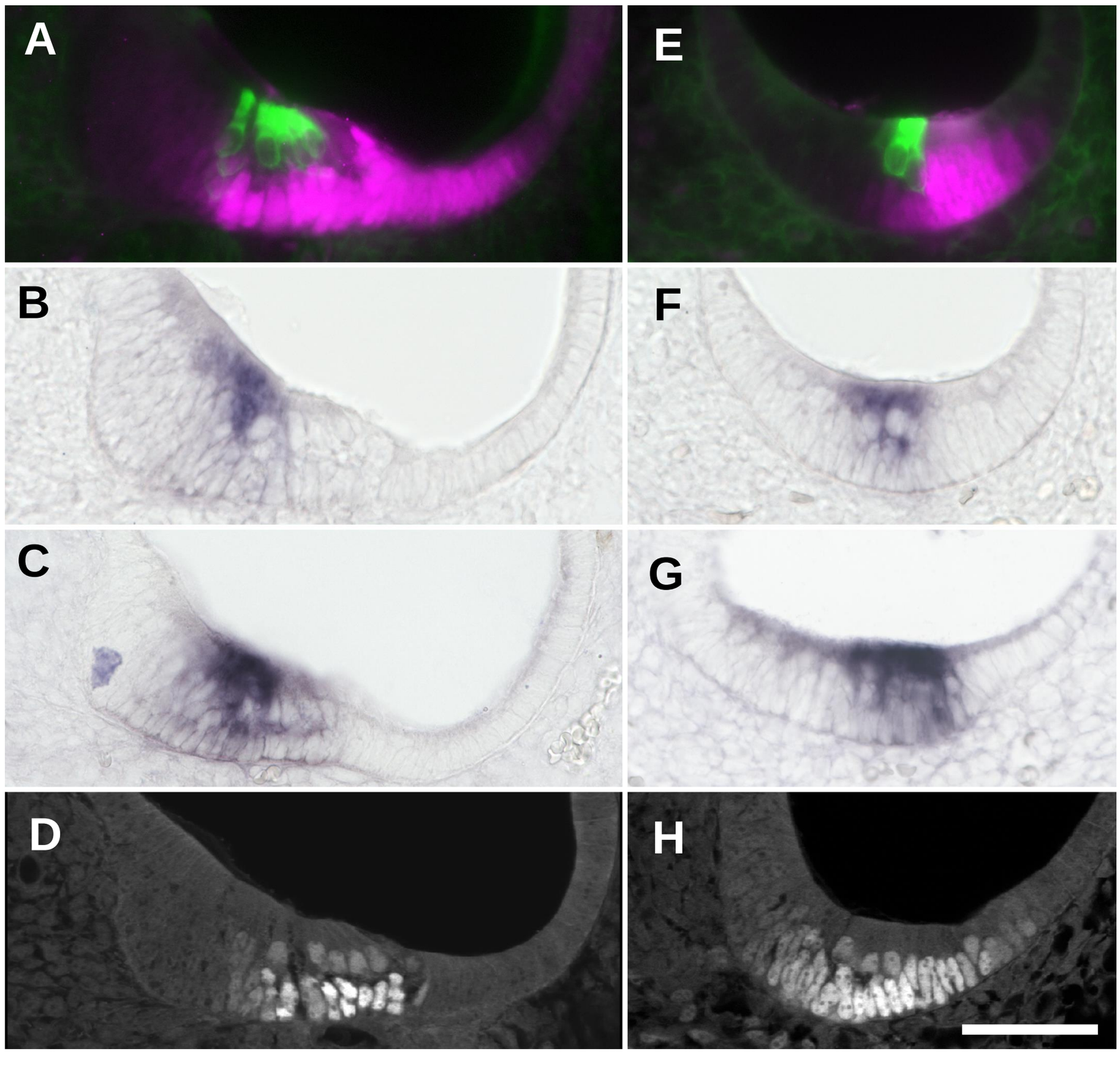

Fgf10

Jag1

Sox2

E16.5 Markers of future outer sulcus

Control | *Id* TKO

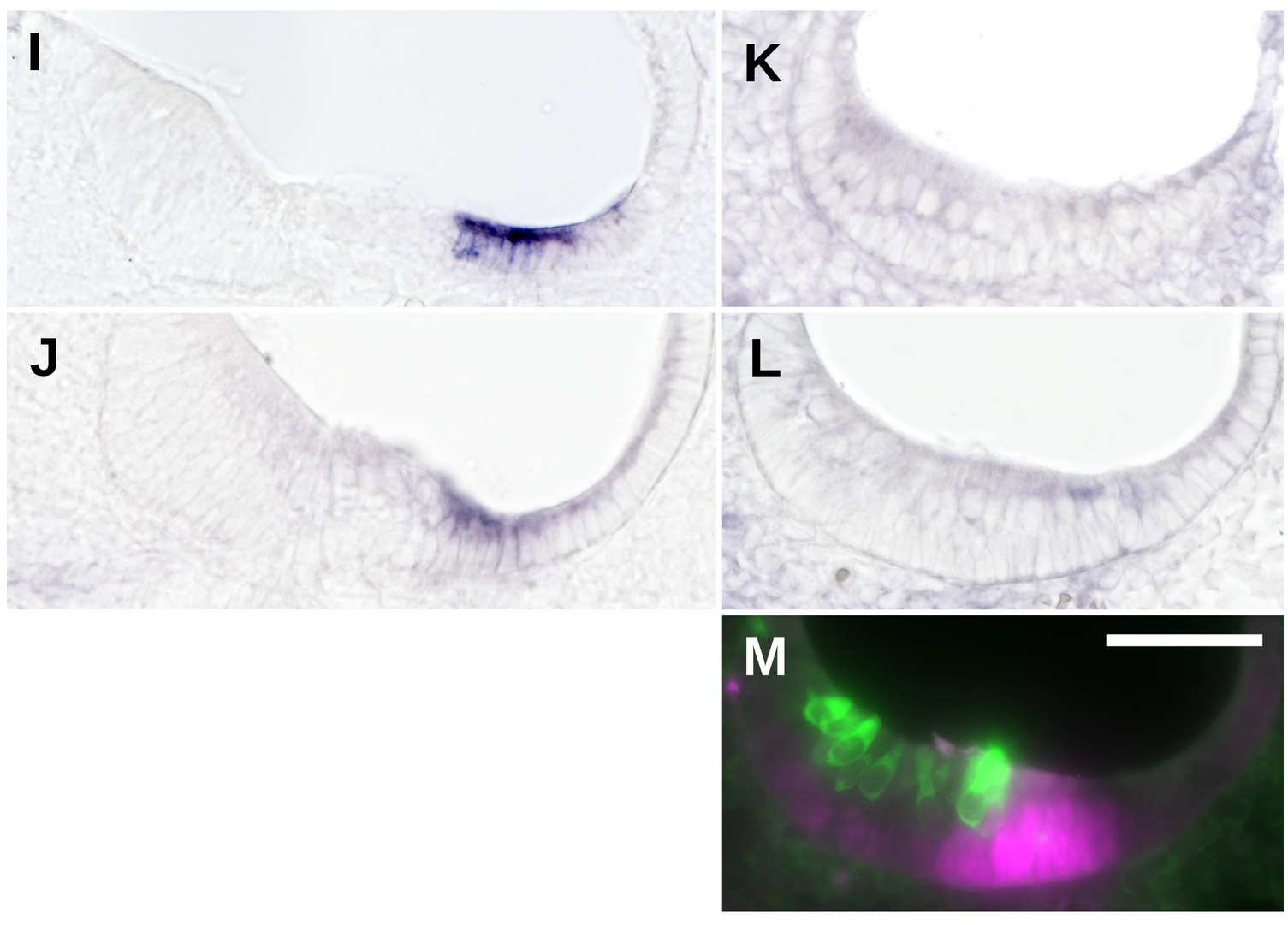

Bmp4

Lmo3

Myosin VI
p27^{Kip1}

Effect of LDN193189 for 24 hours

A

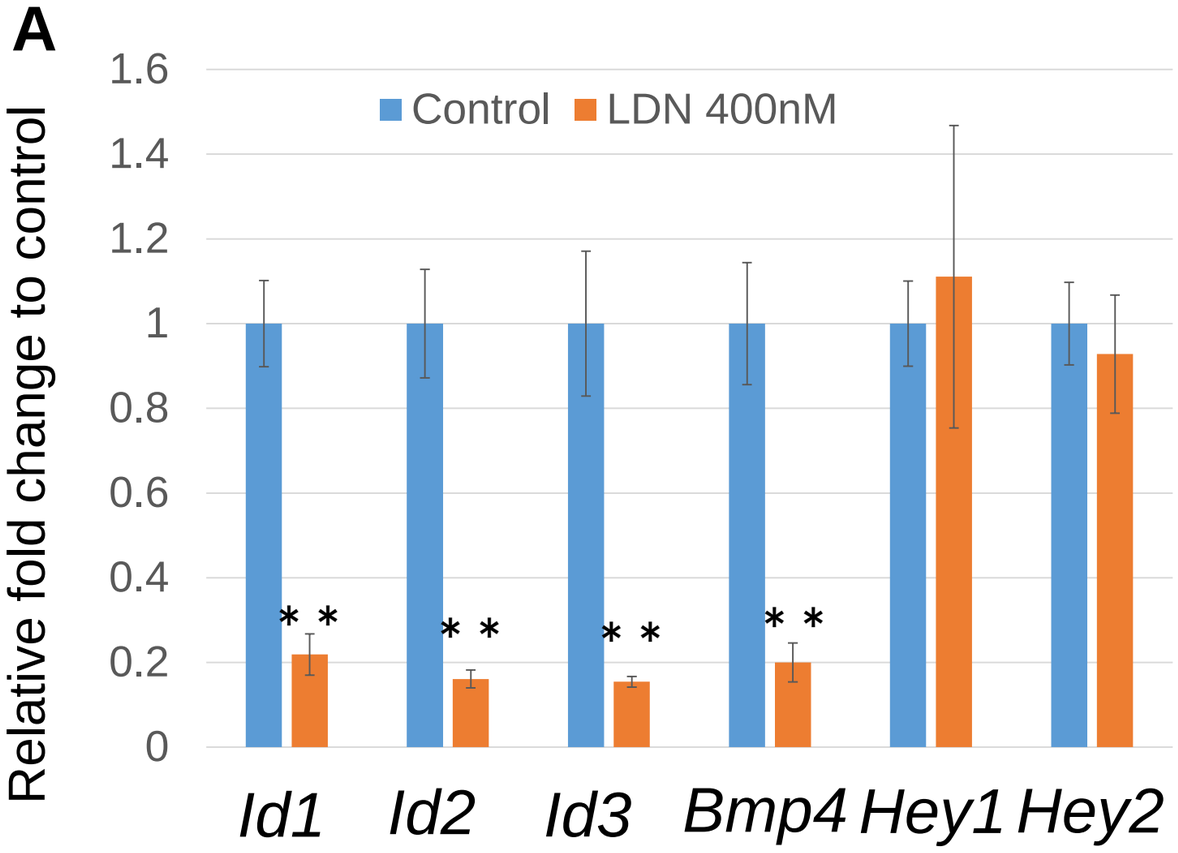

Time Course

B

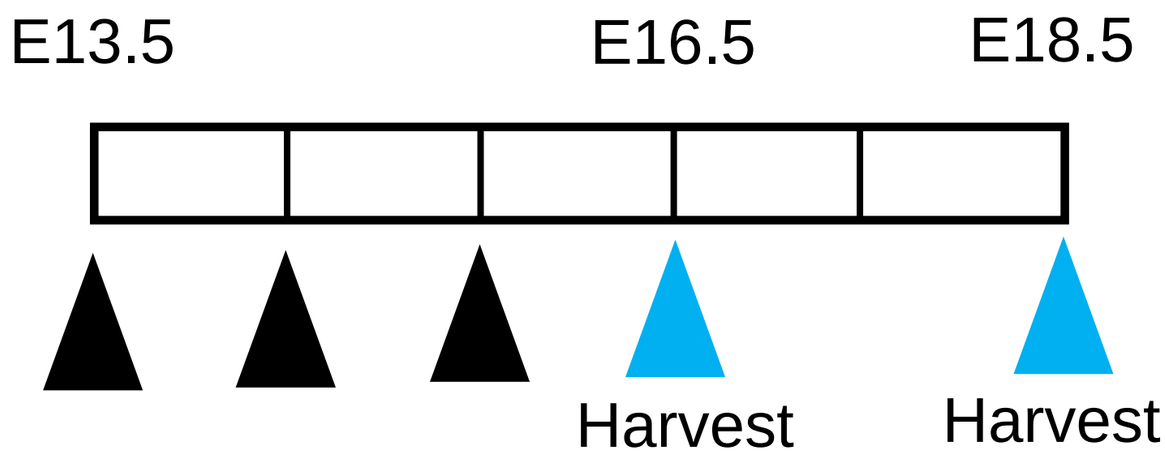

LDN193189 treatment
E13.5- E15.5

3 days culture (MyosinVIIA Sox2)

control	LDN 400nM

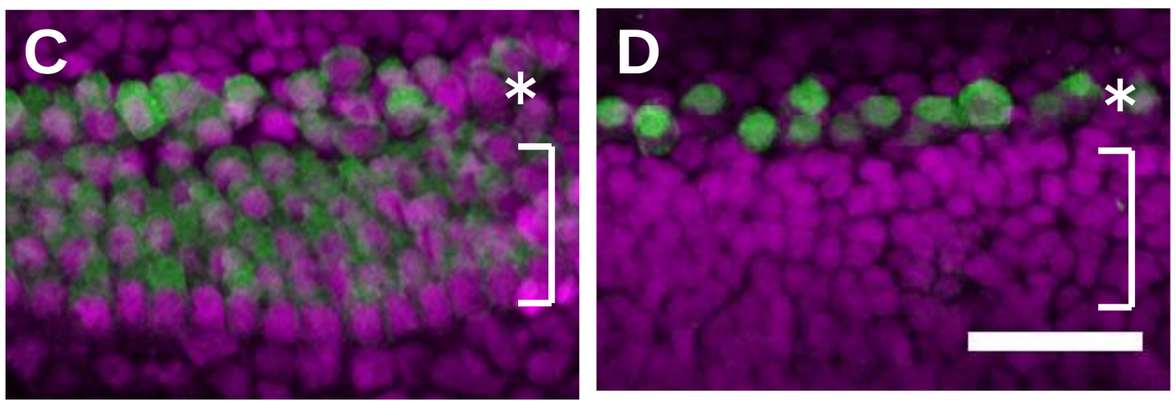

5 days culture

	control	LDN 400nM		control	LDN 400nM
Apical side MyoVIIA p75NTR	E	G	Hair cell layer MyoVIIA Prox1	I	K
Basal side MyoVIIA p75NTR	F	H	Supporting cell layer MyoVIIA Prox1	J	L

Fig. 7

E14.5 *Atoh1* expression

control

Id TKO

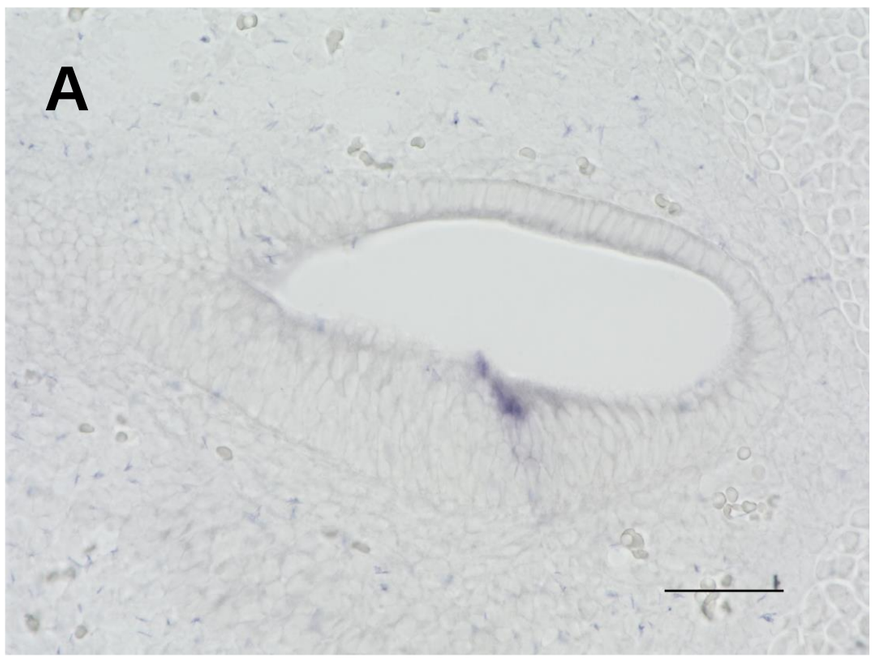

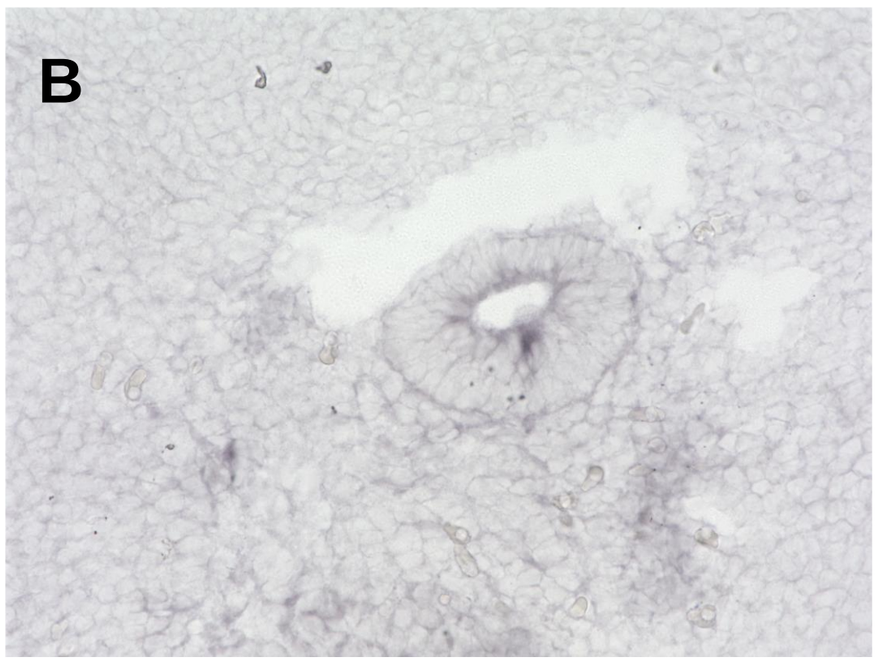

E16.5 *Atoh1* expression

control

Id TKO

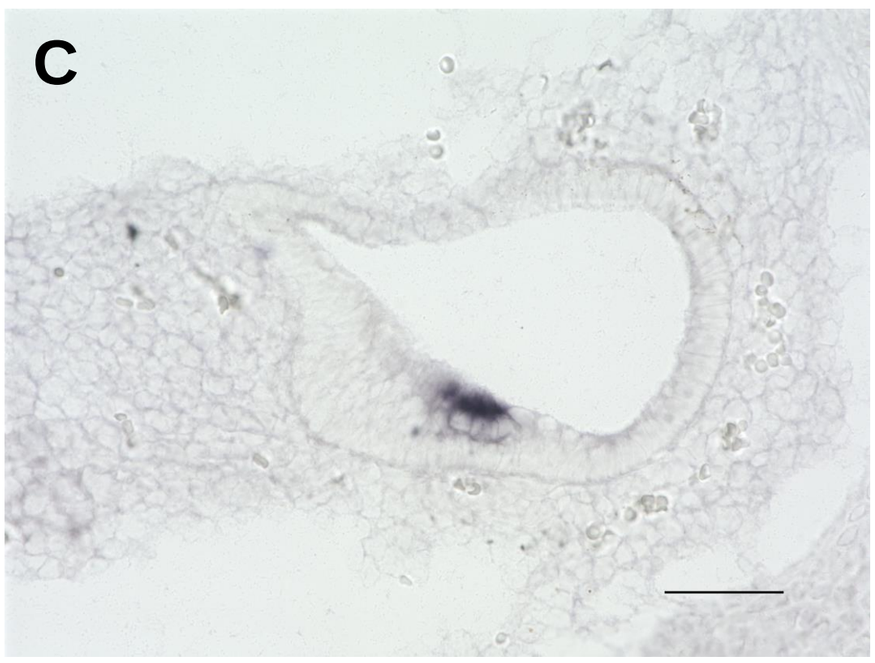

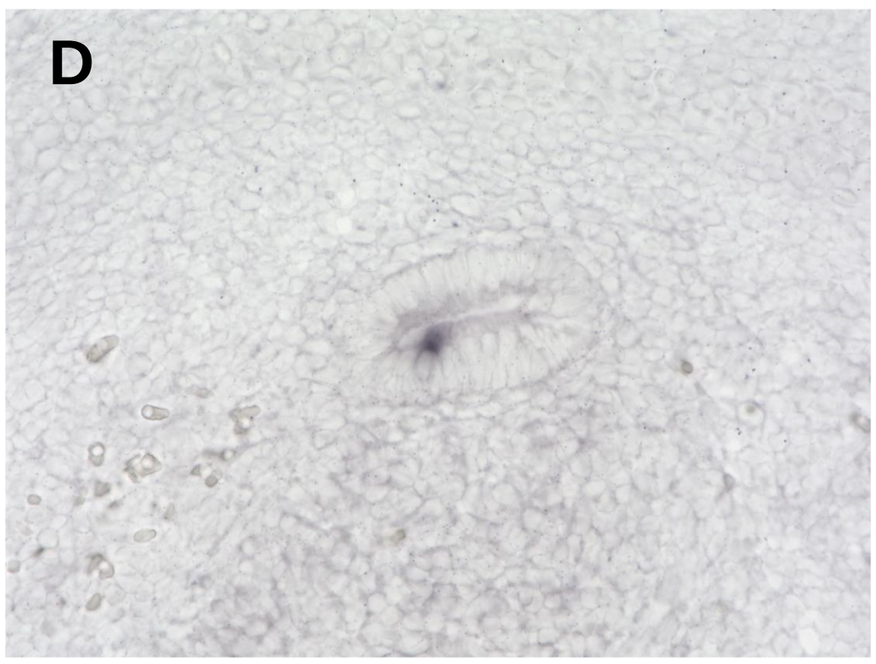

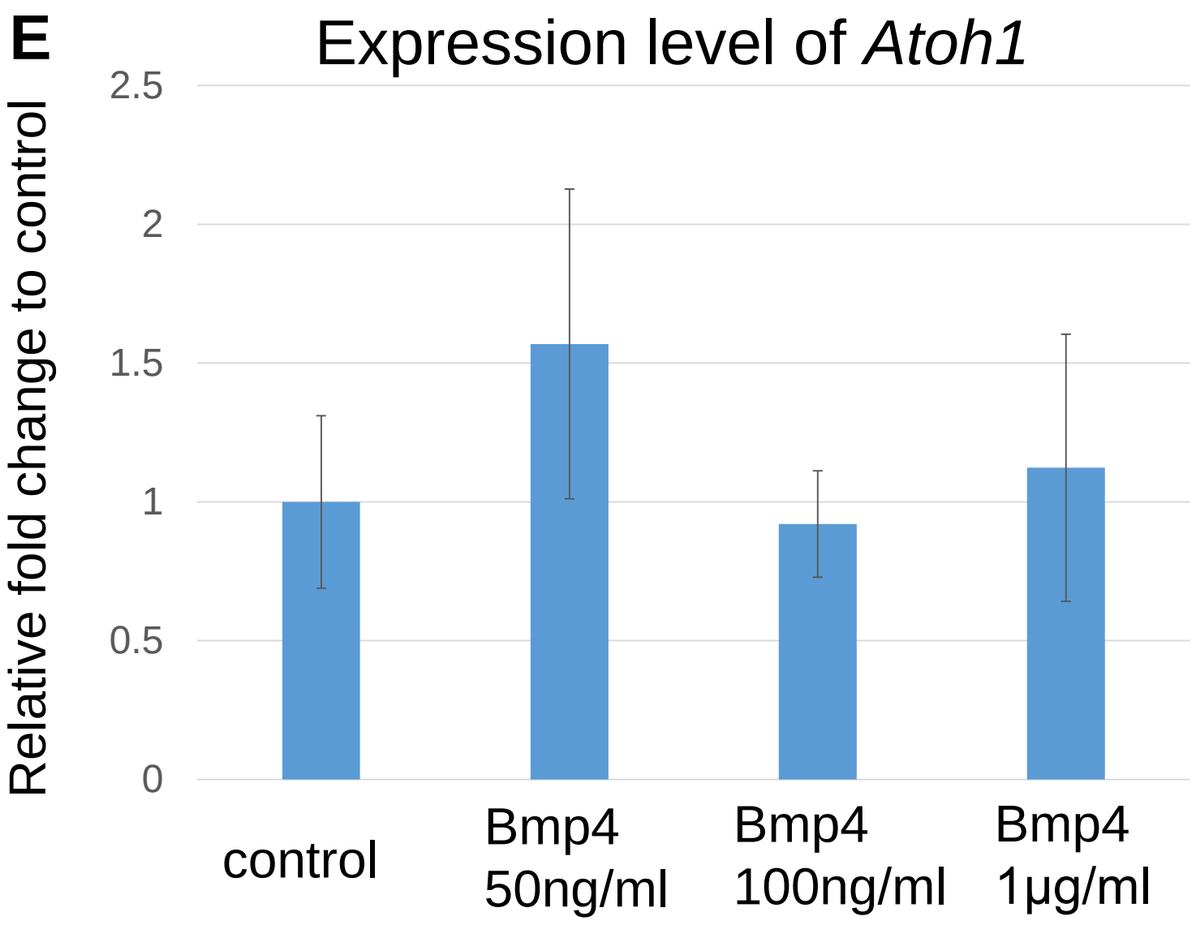

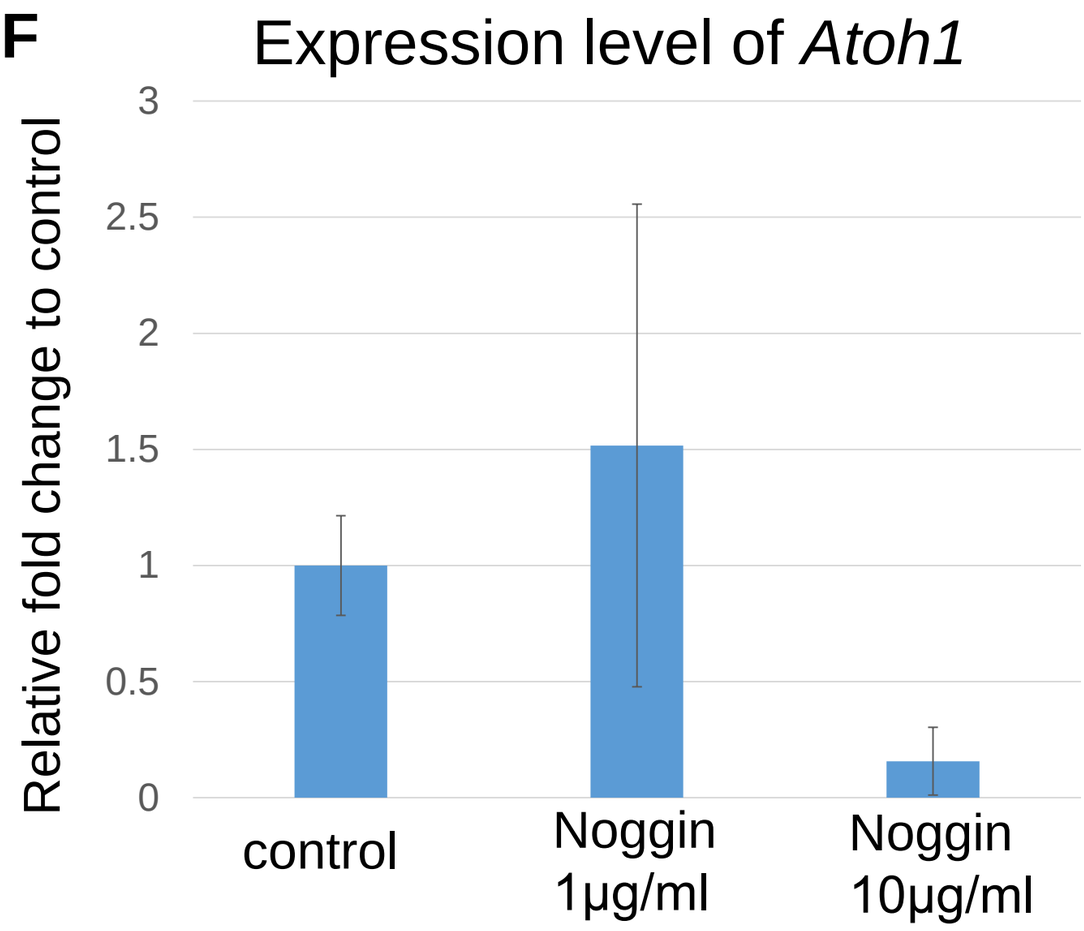

Supporting Information

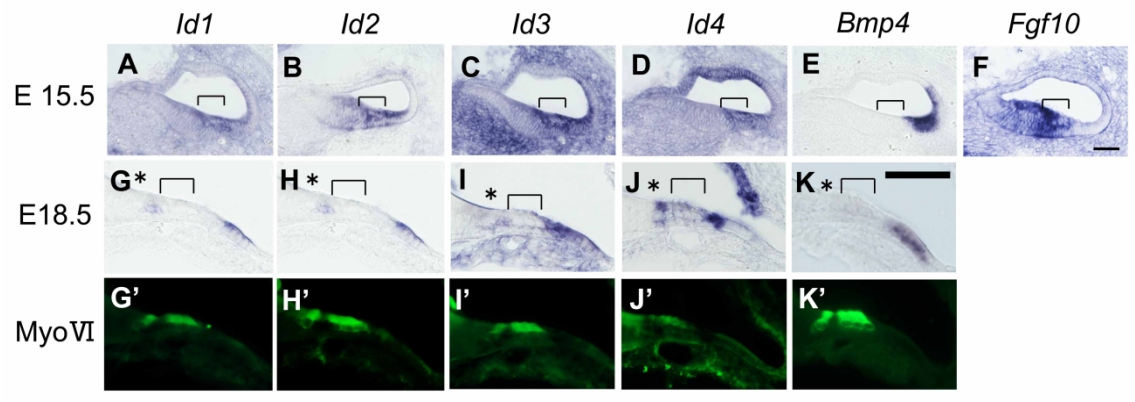

Fig. S1. Expression patterns of *Id1*, *Id2*, *Id3*, and *Id4* at E15.5 and E18.5, related to Fig. 1.

(A–K) Sections at E15.5 (A–F) and E18.5 (G–K) from wild-type cochlear duct. *In situ* hybridization for *Id1* (A, G), *Id2* (B, H), *Id3* (C, I), *Id4* (D, J), *Bmp4* (E, K), and *Fgf10* (F). *Id1–4* were expressed in the developing organ of Corti at E15.5. Brackets indicate the developing organ of Corti in A–F. *Id1–4* expression was restricted in supporting cells at E18.5. (G'–K') Immunohistochemistry for myosin VI (green, MyoVI). The images of G'–K' are the same sections as shown in G–K, respectively. Asterisks indicate IHCs and brackets indicate OHCs in G–K. Scale bars, 50 μm.

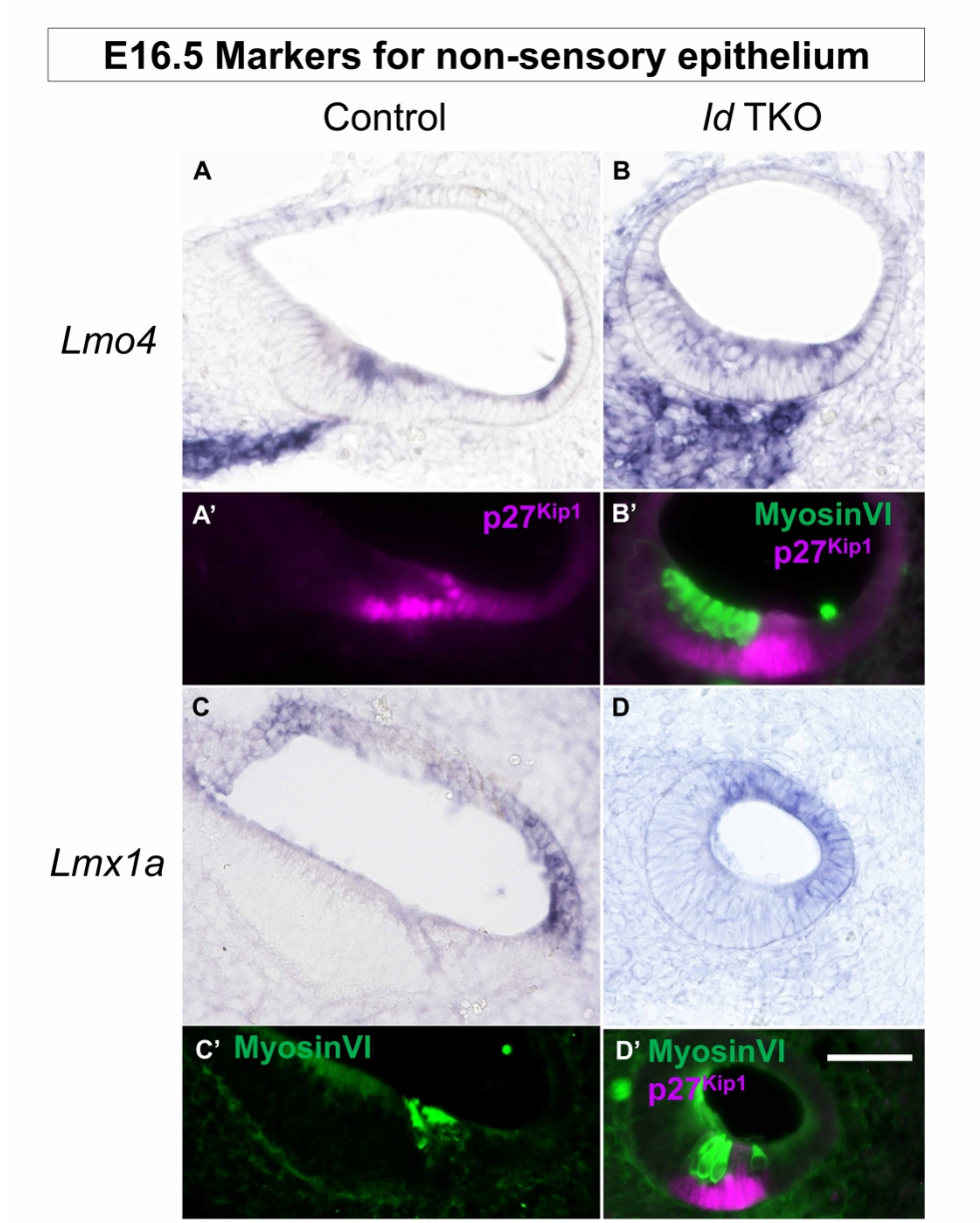

Fig. S2. The non-sensory markers *Lmo4* and *Lmx1a* are detected in E16.5 *Id* TKO cochlea, related to Fig. 6.

Control (A, A', C, C') and *Id* TKO (B, B', D, D') cochleae were analyzed by *in situ* hybridization for *Lmo4* (A, B) and *Lmx1a* (C, D). Expression patterns of the hair cell marker myosin VI (green) and the prosensory and supporting cell marker $p27^{kip1}$ (magenta) (A'–D') were analyzed by immunolabeling. Images in A'–D' are the same sections as shown in A–D, respectively. In the control cochlea, *Lmo4* was expressed in the GER, developing hair cells, and non-sensory domain, which lies at the lateral wall of the cochlear duct, but not in the $Bmp4^{+}$ non-sensory domain. *Lmo4* was expressed throughout the floor of the *Id* TKO cochlear duct, suggesting that *Id* TKO cochlea lacked a $Bmp4^{+}$ lateral non-sensory compartment. *Lmx1a* was expressed in the non-sensory compartment at the roof of the control cochlear duct. In *Id* TKO cochlea, *Lmx1a* expression was maintained. Scale bar, 50 μm (D').

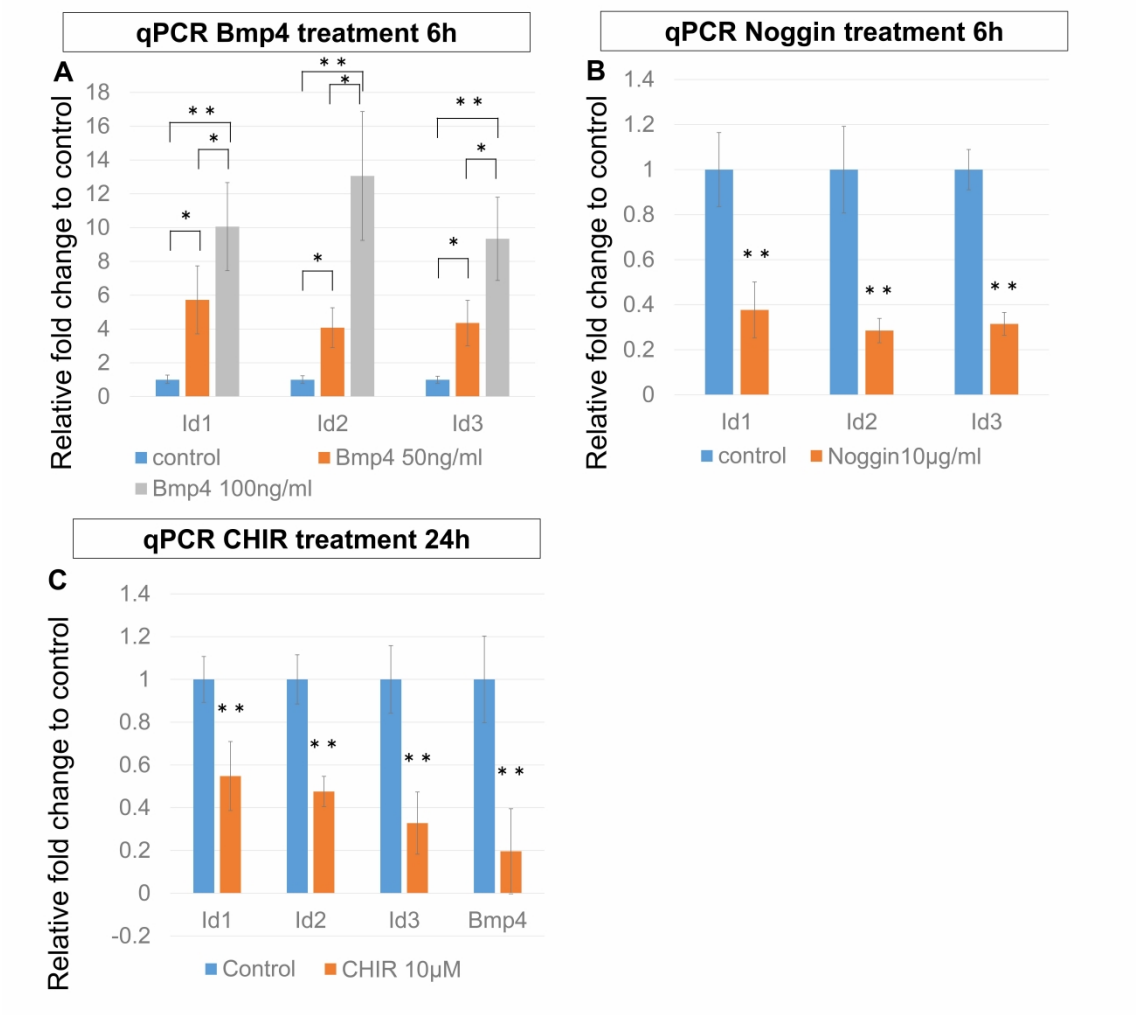

Fig. S3. *Id1*, *Id2*, and *Id3* are positively regulated by Bmp signaling, but negatively regulated by Wnt signaling, in E13.5 cochlear epithelium, related to Fig. 1.

(A) *Id1*, *Id2*, and *Id3* mRNA levels in E13.5 cochlear explants cultured for 6 h with 50 or 100 ng/ml Bmp4 detected by RT-qPCR. The levels are shown as a ratio to control. The expression levels of *Id1*, *Id2*, and *Id3* were upregulated in cochlear explants cultured with Bmp4 in a dose-dependent manner. (B) *Id1*, *Id2*, and *Id3* mRNA levels in E13.5 cochlear explants cultured for 6 h with 10 μg/mL Noggin detected by RT-qPCR. The levels are shown as a ratio to control. The expression levels of *Id1*, *Id2*, and *Id3* were downregulated in cochlear explants cultured with Noggin. (C) *Id1*, *Id2*, *Id3*, and *Bmp4* mRNA levels in E13.5 cochlear explants cultured for 24 h with 10 μM CHIR99021 (CHIR, Wnt activator) detected by RT-qPCR. The levels are shown as a ratio to control. The transcripts of *Id1*, *Id2*, *Id3*, and *Bmp4* were downregulated in cochlear explants cultured with CHIR. *$p < 0.05$, **$p < 0.01$, Student t test.

A Go categories downregulated in *Id* TKO

Go term	p-value
positive regulation of neural precursor cell proliferation	7.98076E-06
response to BMP	5.69318E-05
cellular response to BMP stimulus	5.69318E-05
neural precursor cell proliferation	8.27226E-05
regulation of BMP signaling pathway	0.000128029
epithelial cell proliferation	0.00024087
positive regulation of morphogenesis of an epithelium	0.000270641
epithelial cell differentiation	0.000271831

B Bmp antagonist in *Id* TKO

Gene_ symbol	Base Mean	Log2Fold Change	p-value
Chrd	151.972	0.531	0.113
Sostdc1	549.704	0	1
Nog	131.872	-2.478	0
Fst	736.122	-3.87	0
Grem1	77.245	3.765	0.039

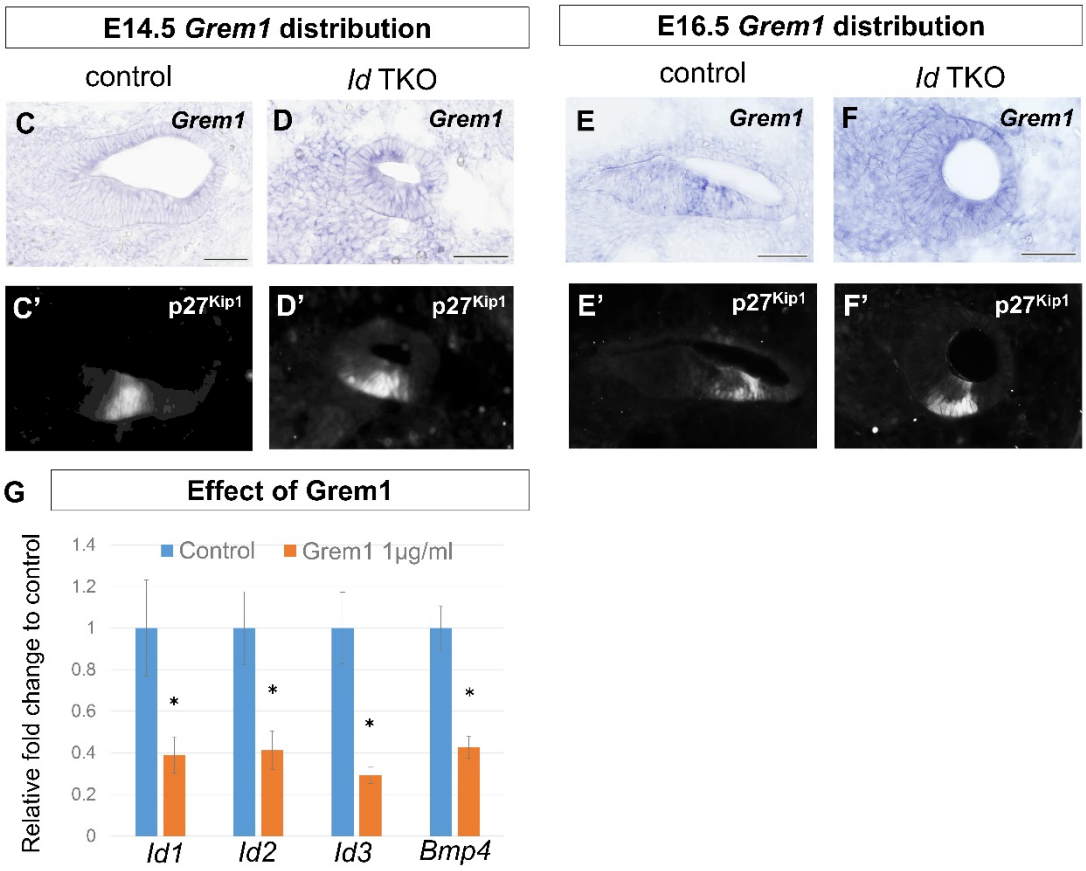

Fig. S4. Inhibition of Bmp4 pathway and upregulation of Grem1 expression in *Id* TKO cochlear epithelium, related to Figs. 2-4.

(A) A table showing representative GO categories for RNA-Seq data of downregulated genes in *Id* TKO cochlear epithelium. Proliferation, differentiation, and Bmp pathway-related categories were downregulated in *Id* TKO cochlear epithelium.

(B) A table of RNA-Seq data analysis showing Bmp signaling pathway-related genes affected in *Id* TKO cochlear epithelium compared with control. Grem1 expression was significantly upregulated in *Id* TKO cochlea.

(C–F, C–F') The expression patterns of Grem1 detected by *in situ* hybridization and p27kip1 detected by immunolabeling are shown. Representative cross sections of the mid-basal turn at E14.5 and E16.5 in control (C, C', E, E') and *Id* TKO (D, D', F, F') cochleae are shown. C'–F' are the same sections as shown in C–F, respectively. Grem1 expression was upregulated in Id TKO cochlea at E14.5 and E16.5. Scale bars, 50 μm.

(G) The mRNA levels of *Id1*, *Id2*, *Id3*, and *Bmp4* in E13.5 cochlear explants cultured for 6 h with or without 1 μg/ml recombinant Grem1 were detected by RT-qPCR. The levels are shown as a ratio to control. The expression levels of *Id1*, *Id2*, *Id3*, and *Bmp4* were downregulated in cochlear explants cultured with recombinant Grem1. *$p<0.05$, Student t test.

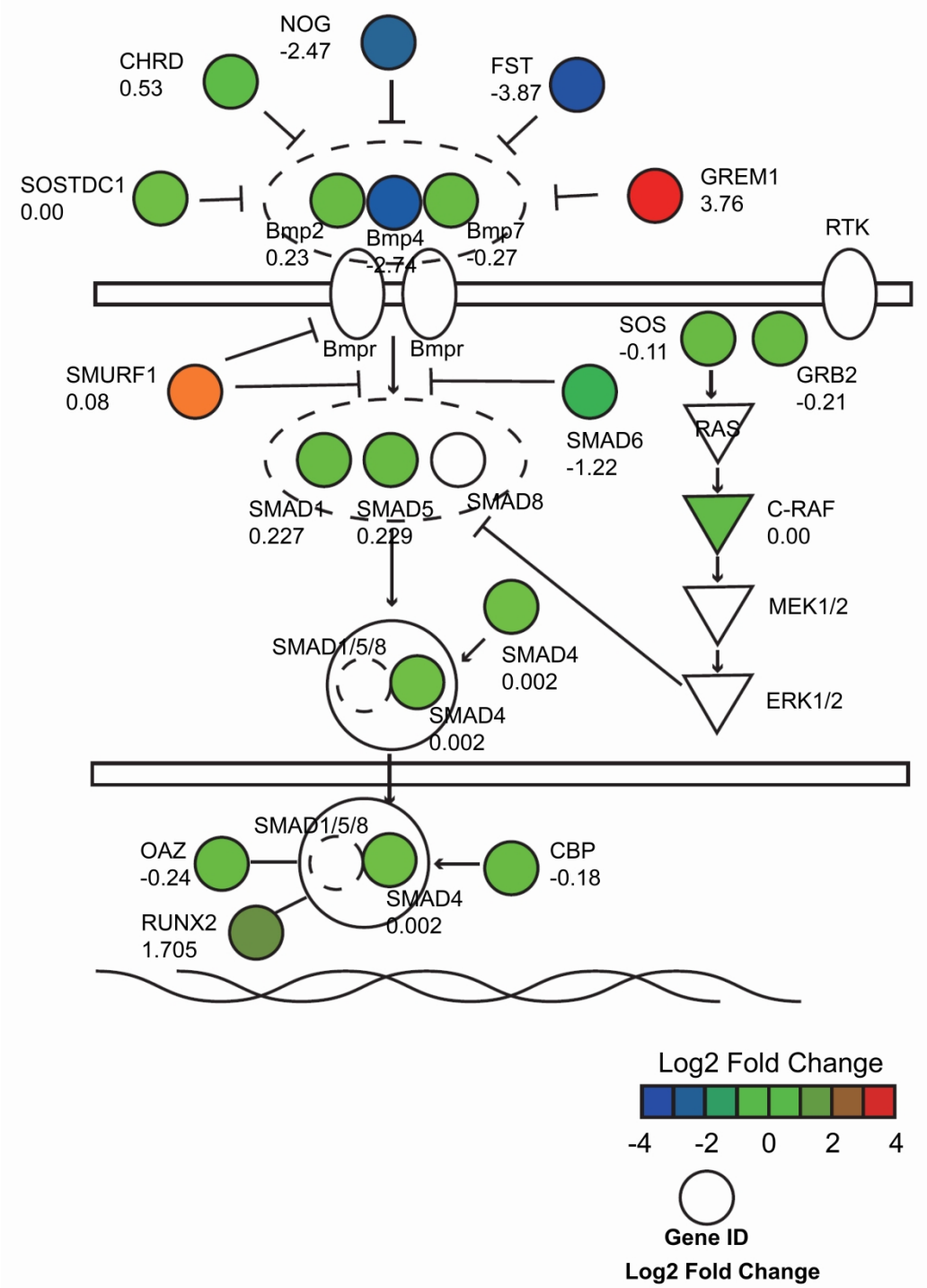

Fig. S5. Pathway analysis of RNA-Seq data in E16.5 control and *Id* TKO cochlear epithelium, related to Fig 7.

Bmp signaling pathway from Ingenuity Pathway Analysis. E16.5 *Id* TKO and control cochlear epithelial tissues were used for RNA-Seq. Genes in green and red are under- and over-expressed, respectively, in *Id* TKO cochlear epithelium. Bmp pathway-related genes were downregulated in *Id* TKO cochlear epithelium. The Bmp antagonist *Grem1* was upregulated significantly in *Id* TKO cochlear epithelium.

Movies

Movie 1. Whole-mount E18.5 control cochleae, related to Fig. 2J.

Movie 1 is the representative image of surface-prepared whole-mount E18.5 control cochlea labeled by anti-E-Cadherin antibody (green) and anti-Sox2 antibody (magenta), and the same as shown in Fig. 3J. Three-dimensional images are rotated vertically and then horizontally.

Movies 2 and 3. Whole-mount E18.5 *Id*-TKO cochleae, related to Fig. 2K, L.

Movies 1 and 2 are the representative images of whole-mount E18.5 *Id*-TKO cochleae labeled by anti-E-Cadherin antibody (green) and anti-Sox2 antibody (magenta), and the same as shown in Fig. 3K and 3L, respectively. Three-dimensional images are rotated vertically and then horizontally.

Movie 4. Whole-mount E18.5 control cochleae, related to Fig. 3A.

Movie 4 is the representative image of surface-prepared whole-mount E18.5 control cochlea labeled by anti-E-Cadherin antibody (green) and anti-$p75^{NTR}$ antibody (magenta), and the same as shown in Fig. 3A. Three-dimensional images are rotated vertically and then horizontally.

Movie 5. Whole-mount E18.5 *Id*-TKO cochlea, related to Fig. 3B, C.

Movie 5 is the representative image of whole-mount E18.5 *Id*-TKO cochlea labeled by anti-E-Cadherin antibody (green) and anti-$p75^{NTR}$ antibody (magenta), and the same as shown in Fig. 3B, C. Three-dimensional images are rotated vertically and then horizontally.